Vietnam National University Ho Chi Minh City
University of Science
Faculty of Physics
Department of Theoretical Physics

ICISE, Quy Nhon, Vietnam
Institute For Interdisciplinary Research in Science and Education
Theoretical Physics Group

———————— * ————————

BACHELOR THESIS

HARD-PHOTON CORRECTIONS TO ELECTRON MUON ELASTIC SCATTERING IN QED

Le Van Cuong

Supervisor: Dr. Le Duc Ninh
Reviewer: Dr. Phan Hong Khiem

HO CHI MINH CITY - 2021

ACKNOWLEDGEMENTS

First of all, I would like to express my deepest appreciation to my supervisor Dr. Le Duc Ninh for his unfailing help and guidance, generosity over my failure to meet the deadlines. His scientific spirit motivates extremely not only me but also other students. I also gratefully acknowledge helpful conversations with him which have helped to improve my understanding.

I am grateful to Prof. Jean Tran Thanh Van for giving me an opportunity to do this internship and enjoy the scientific environment at Institute For Interdisciplinary Research in Science and Education (IFIRSE).

From the department of theoretical physics at the University of Science, several lessons and seminars helped me so much to better understand the basis of physics and problems solving. The lectures about the theory of Solid and Optical Semiconductors giving by Dr. Vu Quang Tuyen make me have a new standpoint and helped me to learn how to decay the realistic problems into simpler ones. Sir. Dang Ngoc Chau shows me the beauty and mystery of mathematics. I also thank Dr. Vo Quoc Phong - a big brother. He builds many creative lessons about the laws of physics and has an incredible point of views.

I would like to extend my sincere thanks to Dr. Phan Hong Khiem, my Quantum Field Theory and Elementary Physics lecturer, for being the reviewer of this thesis. He helped me to realize how beautiful the Standard Model is and taught me how to investigate the microscopic world of particles.

For the staff members at IFIRSE, I would like to thank Dr. Dao Thi Nhung and MSc. Nguyen Hoang Duy Thanh for their advice and suggestions helping me to overcome the challenging problems in my thesis.

I would also like to extend my gratitude to all my friends in the 17^{th} theoretical physics class: Man Hoang Que, Vu Cong Ngoc Thai, Tran Ngoc Thien, Nguyen Huy Hien, Nguyen Xuan Vinh, Le Van Dung, Tran Thi Minh Hoan, Nguyen Hoang Tuan Dat, Nguyen Thi Nhung and Le Hoang Buu for their constant good humor and patience that cannot be underestimated.

Finally, I am particularly grateful to my father, Mr. Le Van Pho, who has supported me throughout my long working project with selfless encouragement, love, and understanding.

ABSTRACT

Recently, the MuonE experiment has been proposed as a new method to measure precisely the running of fine-structure electromagnetic coupling in the space-like region via the electron muon elastic scattering. This will help to resolve the $4.2\,\sigma$ discrepancy between the Standard Model prediction and the currently combined experimental measurement for the muon anomalous magnetic moment. For the MuonE experiment, experimentalists require calculating very precisely the cross-section of the electron muon elastic scattering at next-to-next-to-leading order. Therefore, evaluating the cross-section at next-to-leading order is a prerequisite to achieve this requirement. In this thesis, we calculate the hard-photon corrections to the cross-section of the electron muon elastic scattering via the bremsstrahlung process $e\mu \to e\mu\gamma$ and combine with the known virtual and soft-photon corrections to obtain the full next-to-leading order results, utilizing the high-precision Monte-Carlo programs VEGAS+ and BASES for numerical calculation.

INTRODUCTION

The MUonE experiment has been proposed as a new method to estimate the running effective electromagnetic coupling constant at space-like region via the process of muon-electron elastic scattering by using a muon beam at 150 GeV scatter on atomic electron at a low-Z target [1]. The differential cross-section of this process provides the direct measurement of the leading-order hadronic contribution to the muon anomalous momenta, $a_\mu^{\rm HLO}$, which is a test of the Standard Model (SM) prediction of particle physics [2]. The experiment plans have been currently prepared at Fermilab [3] (USA) and J-PARC [4] (Japan), aiming to measure the muon anomaly at a precision of 0.14 ppm [3, 5]. To achieve such high precision, the experimentalists require the theoretical calculation the differential cross-section of $e\mu$ scattering at next-to-next-to-leading order (NNLO) at 10 ppm [1]. The first step toward the calculation at high-order is evaluated very precisely at the next-to-leading order (NLO) in the framework of SM due to Quantum Electrodynamics (QED) and electroweak contributions. The previous study at full set of leading-order (LO) and NLO QED soft-photon corrections was presented in Le Duc Truyen's thesis "Electron muon elastic scattering in one-loop QED with soft-photon corrections" [6]. A full calculation at NLO had been published by Alacevich et al [7].

In this thesis, we calculate the NLO QED hard-photon corrections via bremsstrahlung process $\mu e \to \mu e \gamma$. At a high level of accuracy, the mass of the electron must be kept without any approximations and for obtaining the cross-section, the high-precision computer programs are necessary. Monte-Carlo integration programs BASES [8], VEGAS+ [9, 10] are used in our work. The hard-photon corrections calculated here will be combined with the virtual and soft-photon corrections from Ref. [6] to obtain the full NLO QED results. The thesis is organized as follows:

- **Chapter 1: An overview of QED**
  We briefly describe the QED theory (focusing on the Lagrangian of QED) and Feynman rules, aiming to prepare the theoretical framework for posterior chapters.

- **Chapter 2: Phase space of N particles**
  We present and discuss the integration of phase space element of an N-particle scattering process. Then, we illustrate how to generate the momentum configuration in terms of geometric and kinematical variables.

- **Chapter 3: Bremsstrahlung process $e\mu \to e\mu\gamma$ in QED**
  We derive the Feynman amplitude of the reaction $e\mu \to e\mu\gamma$ and calculate the cross-section with a cut-off kinematic condition in the hard-photon region. Besides, the experiment requires that the energy of the outgoing electron must be greater than 0.2 [GeV] in the laboratory frame. Finally, we present the full NLO results.

- **Chapter 4: Conclusion and Outlook**
  We summarize our work.

CONTENTS

LIST OF FIGURES

LIST OF TABLES

CHAPTER

ONE

AN OVERVIEW OF QED

1.1 The Lagrangian of QED

Long time ago, the question from the physical standpoint is "How light and matter interact with each other and how to describe them in the framework of quantum mechanics at very high velocities considerable ?". With the born of Quantum Electrodynamics (QED) theory this question is answered which agrees well between quantum mechanics and special relativity (theory for the particles moving with velocity approximate the velocity of light). It gives very accuracy predictions for quantities like the energy level in hydrogen atom or behavior of charged particles at microscopic region. In the search for new physics, the new theory must agree with QED predictions at the low energy scale.

Quantum Electrodynamics associates with the electromagnetic interaction, the fermion field $\psi(x)$ with the mass m and the massless photon field $A_\mu(x)$. The Lagrangian density (or the Lagrangian, for short) of this model [11] is:

$$\mathcal{L}_{\rm QED}(x) = \bar{\psi}(x)(i\gamma^\mu\partial_\mu - m)\psi(x) - \frac{1}{4}F_{\mu\nu}F^{\mu\nu} - e\bar{\psi}(x)\gamma^\mu\psi(x)A_\mu(x). \tag{1.1}$$

We consider only the case of charged leptons l ($l = e, \mu$). In the Lagrangian (1.1), the first term describes the kinematic of the fermion field, the second term is the kinematic of the photon field, with an electromagnetic field tensor: $F_{\mu\nu} = \partial_\mu A_\nu - \partial_\nu A_\mu$.

The existence of the interaction term (the last term) in Eq. (1.1) is prerequisite for deriving scattering amplitude which gives information about the transition probability of the scattering process. The Wick theorem has been used as an intermediate procedure after expanding the S-matrix element (technical details can be found in Appendix A). Differently from the Wick theorem, another common technique for evaluating the amplitude is an intuitive mathematics approach via a pictorial representation named Feynman diagram, which was invented by the American physicist Richard Feynman.

In the next section, we present the Feynman rules of QED.

1.2 Feynman rules in QED

1.2.1 External line

Each external line includes the coefficient:

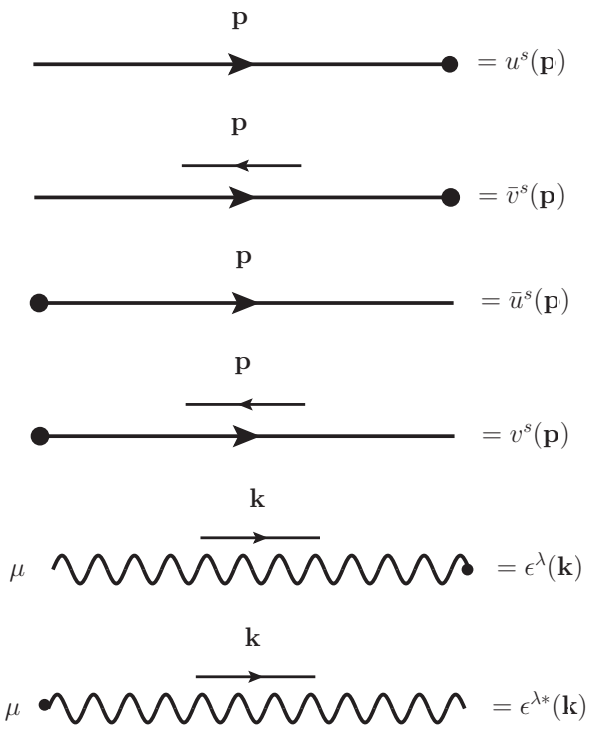

where s represents spin index, $\mathbf{p}$ is the three-momentum of the fermion, λ and $\mathbf{k}$ correspond to polarization index and the three-momentum of the photon, respectively.

1.2.2 Interaction Vertex

From the interaction term $\mathcal{L}_{\text{int}}$ in the Lagrangian (1.1), we can use the peeling-method to remove all field operators for obtaining the interaction vertex.

$$\mathcal{L}_{\text{int}} = -e\bar{\psi}(x)\gamma^{\mu}\psi(x)A_{\mu}(x). \tag{1.2}$$

The interaction vertex reads:

$$\frac{\partial}{\partial(A_{\mu}(x)\bar{\psi}(x)\psi(x))}(i\mathcal{L}_{\text{int}}) = -ie\gamma^{\mu}. \tag{1.3}$$

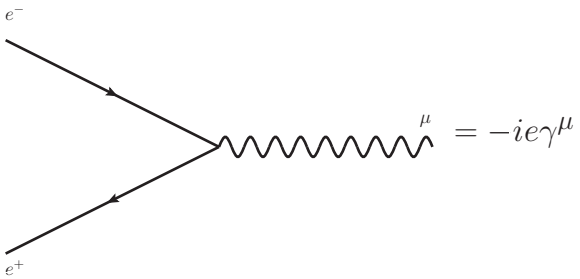

At each vertex, the energy-momentum and electric-charge conservations must be satisfied.

1.2.3 Propagator

1. For each internal photon line, it associates with the photon propagator:

$$D^F_{\mu\nu}(q) = \frac{-ig_{\mu\nu}}{q^2 + i\epsilon}. \tag{1.4}$$

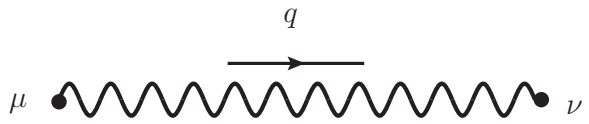

Figure 1.1: Photon propagator.

2. For each internal fermion line, it associates with the fermion propagator:

$$S^F_{\alpha\beta}(p) = \left[\frac{i(\not{p} + m)}{p^2 - m^2 + i\epsilon}\right]_{\alpha\beta}, \tag{1.5}$$

where α, β are called Dirac indices.

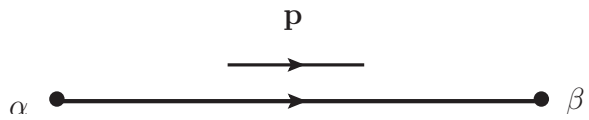

Figure 1.2: Fermion propagator.

CHAPTER

TWO

PHASE SPACE OF N PARTICLE SCATTERING

In the present chapter, we focus on the definition of phase space and the most important quantity in the reaction processes which is the total cross-section. At the end of this chapter, we perform the technical steps to generate a set of momentum configurations in terms of kinematical and geometric variables.

As an usual formalism in the dynamics study of a particle reaction, the conservation laws must be hold.
For the $2 \to n$ scattering with $n = N - 2$, $p_1 + p_2 \to p_3 + \ldots + p_N$, we have:

$$E_1 + E_2 = \sum_{i=3}^{N} E_i, \tag{2.1}$$

$$\mathbf{p}_1 + \mathbf{p}_2 = \sum_{i=3}^{N} \mathbf{p}_i, \tag{2.2}$$

where m_i is the rest mass of the particle,

$$E_i^2 = |\mathbf{p}_i|^2 + m_i^2. \tag{2.3}$$

The momentum space is first defined from the $3n$-components of the outgoing momenta. The presence of four-momentum conservation law in this space causes the energy and momenta of the outgoing particles can not vary arbitrarily. Hence, we define the **phase space** with the $3n - 4$ dimensions as a combination of the **momentum space** and the **four-momentum conservation law**. If we consider the initial state of two incoming particles, it is often fixed by an experiment setting and it is called a fixed channel.

For obtaining the measurable quantity in the reaction process $2 \to n$, the square of the transition probability matrix, which we will denote as $|\mathcal{M}|^2$, is integrated with all allowed variables $\mathbf{p}_i$. If the integrals are computed in $3n - 4$ dimensional phase space, the result will be the total reaction cross-section (the total cross-section, for short). The formula of the total cross-section in a fixed channel [12]:

$$\sigma(s) = \frac{1}{Z} R_{2\to n}(s), \tag{2.4}$$

where $\sqrt{s}$ is the total collision energy, $Z = 4\sqrt{(p_1.p_2)^2 - m_1^2 m_2^2}$ is the incoming flux factor and

$$R_{2\to n}(s) = \int (2\pi)^4 \delta^4(P_i - P_f)|\mathcal{M}|^2 \,\mathrm{d}\Phi \tag{2.5}$$

contains the integration over phase space. In Eq. (2.5), P_i, P_f correspond to the total momentum of initial particles and final particles, respectively,

$$P_i = p_1 + p_2, \tag{2.6}$$
$$P_f = p_3 + p_4 + \ldots + p_N. \tag{2.7}$$

Additional, the four-momentum conservation is presented by the four-dimensional delta function $\delta^4(P_i - P_f)$ and the $2 \to n$ phase space element $\mathrm{d}\Phi$:

$$\mathrm{d}\Phi = \frac{\mathrm{d}^3\mathbf{p}_3}{(2\pi)^3 2E_3} \frac{\mathrm{d}^3\mathbf{p}_4}{(2\pi)^3 2E_4} \cdots \frac{\mathrm{d}^3\mathbf{p}_N}{(2\pi)^3 2E_N}. \tag{2.8}$$

The factor $\prod_{i=3}^{N}(2E_i)$ in the denominator of Eq. (2.8) is just for convenience which refers to the fact that the quantity $\mathrm{d}^3\mathbf{p}\,/2E$ is invariant under Lorentz transformation. Considering the Lorentz transformation (Appendix B):

$$\mathrm{d}p_x = \mathrm{d}p'_x\,, \tag{2.9}$$
$$\mathrm{d}p_y = \mathrm{d}p'_y\,, \tag{2.10}$$
$$\begin{aligned}\mathrm{d}p_z &= \gamma(\mathrm{d}p'_z - v\,\mathrm{d}E') \\ &= \gamma\,\mathrm{d}p'_z\,(1 - vp'_z/E') \\ &= \mathrm{d}p'_z\,E/E',\end{aligned} \tag{2.11}$$
$$\Rightarrow \frac{\mathrm{d}p_z}{E} = \frac{\mathrm{d}p'_z}{E'} \tag{2.12}$$
$$\Rightarrow \frac{\mathrm{d}^3\mathbf{p}}{2E} = \frac{\mathrm{d}^3\mathbf{p}'}{2E'}, \tag{2.13}$$

where $\mathrm{d}E'\,/\,\mathrm{d}p'_z = p'_z/E'$ and $E = \gamma(E' - vp'_z)$. Therefore, $\mathrm{d}^3\mathbf{p}\,/2E$ is invariant under the Lorentz transformation. Next, we have:

$$\mathrm{d}^4p = \det(\Lambda)\,\mathrm{d}^4p' \tag{2.14}$$
$$= \det \begin{pmatrix} \frac{\mathrm{d}E'}{\mathrm{d}E} & \frac{\mathrm{d}E'}{\mathrm{d}p_x} & \frac{\mathrm{d}E'}{\mathrm{d}p_y} & \frac{\mathrm{d}E'}{\mathrm{d}p_z} \\ \frac{\mathrm{d}p'_x}{\mathrm{d}E} & \frac{\mathrm{d}p'_x}{\mathrm{d}p_x} & \frac{\mathrm{d}p'_x}{\mathrm{d}p_y} & \frac{\mathrm{d}p'_x}{\mathrm{d}p_z} \\ \frac{\mathrm{d}p'_y}{\mathrm{d}E} & \frac{\mathrm{d}p'_y}{\mathrm{d}p_x} & \frac{\mathrm{d}p'_y}{\mathrm{d}p_y} & \frac{\mathrm{d}p'_y}{\mathrm{d}p_z} \\ \frac{\mathrm{d}p'_z}{\mathrm{d}E} & \frac{\mathrm{d}p'_z}{\mathrm{d}p_x} & \frac{\mathrm{d}p'_z}{\mathrm{d}p_y} & \frac{\mathrm{d}p'_z}{\mathrm{d}p_z} \end{pmatrix} \mathrm{d}^4p' \tag{2.15}$$
$$= \det \begin{pmatrix} \gamma & 0 & 0 & -v\gamma \\ 0 & 1 & 0 & 0 \\ 0 & 0 & 1 & 0 \\ -v\gamma & 0 & 0 & \gamma \end{pmatrix} \mathrm{d}^4p'\,. \tag{2.16}$$

Furthermore, the determinant of the Λ matrix equals to 1, so the d^4p is a Lorentz invariant quantity, and the identities:

$$\int \delta^4(p-q)\,\mathrm{d}^4p = 1, \tag{2.17}$$

$$\int \delta^4(p'-q')\,\mathrm{d}^4p' = 1. \tag{2.18}$$

Besides, the right hand side of Eq. (2.17) and Eq. (2.18) is a number. Hence, the δ^4 function is also the invariant quantity. Consequently, the cross-section in Eq. (2.5) is invariant under the Lorentz transformation and we can choose any specifically frames of reference to compute and obtain the same result.

In Eq. (2.5), if the square of the transition matrix element $|\mathcal{M}|^2$ is one, the integral $R_{2\to n}(s)$ is called the **phase space integral**. The next two sections present some general properties of the phase space integral in different cases: two and three final particles.

2.1 Two-particle final states

2.1.1 Decay process

To begin with, we first consider a decay process: one particle decays into two particles $(1 \to 2)$ in the rest frame of p_1 which is defined as a frame where the spatial components of initial particle are zero $p_1 = (E_1, \mathbf{p}_1) = (E_1, 0)$.

$$p_1 \to p_2 + p_3 \tag{2.19}$$

We have the invariant mass squared s_1 defined from the total four-momentum $p_1^0 = E_1$ of the initial particle:

$$s_1 \equiv p_1^2 = (p_2+p_3)^2 \tag{2.20}$$

$$= E_1^2 = (E_2+E_3)^2. \tag{2.21}$$

Phase space integral is defined as:

$$R_{1\to2}(s_1, m_2^2, m_3^2) = \int (2\pi)^4\delta^4(p_1-p_2-p_3)\frac{\mathrm{d}^3\mathbf{p}_2}{(2\pi)^3 2E_2}\frac{\mathrm{d}^3\mathbf{p}_3}{(2\pi)^3 2E_3}. \tag{2.22}$$

Replacing the three-dimensional momentum to the four-dimensional one by using the relation [11]:

$$\frac{\mathrm{d}^3\mathbf{p}_3}{(2\pi)^3 2E_3} = \frac{\mathrm{d}^4p_3}{(2\pi)^4}(2\pi)\delta(p_3^2-m_3^2)\Theta(E_3). \tag{2.23}$$

The theta function $\Theta(E_3)$ has value 1 if $E_3 \geq 0$ and equals to 0 if $E_3 < 0$. This kind of function appears in all expressions of $R_{1\to2}$. We substitute Eq. (2.23) into Eq. (2.22) and consider $E_3 \geq 0$. Hence, the phase space integral of the decay process is:

$$R_{1\to2}(s_1, m_2^2, m_3^2) = \int (2\pi)^4\delta^4(p_1-p_2-p_3)\frac{\mathrm{d}^3\mathbf{p}_2}{(2\pi)^3 2E_2}\frac{\mathrm{d}^4p_3}{(2\pi)^3}\delta(p_3^2-m_3^2). \tag{2.24}$$

Integrating Eq. (2.24) over p_3 by using the four-dimensional delta function and implement $p_3 = p_1 - p_2$ in Eq. (2.25).

$$R_{1\to2}(s_1, m_2^2, m_3^2) = \frac{1}{(2\pi)^2}\int \frac{\mathrm{d}^3\mathbf{p}_2}{2E_2}\delta[(p_1 - p_2)^2 - m_3^2]. \tag{2.25}$$

In the spherical coordinates, we have $\mathrm{d}^3\mathbf{p}_2 = |\mathbf{p}_2|^2\,\mathrm{d}|\mathbf{p}_2|\,\mathrm{d}\Omega_{12}$ with $\Omega_{12} = (\cos\theta_{12}, \phi_{12})$ is a solid angle of $\mathbf{p}_2$ orientations in the rest frame of p_1 and get:

$$R_{1\to2}(s_1, m_2^2, m_3^2) = \frac{1}{(2\pi)^2}\int \frac{|\mathbf{p}_2|^2\,\mathrm{d}|\mathbf{p}_2|\,\mathrm{d}\Omega_{12}}{2E_2}\delta(p_1^2 + p_2^2 - 2E_1E_2 - m_3^2). \tag{2.26}$$

Using the on-shell condition (2.27) and taking the derivative of both sides, we obtained the differential relation of energy and momentum:

$$E_2^2 = |\mathbf{p}_2|^2 + m_2^2 \tag{2.27}$$

$$\Rightarrow |\mathbf{p}_2|\,\mathrm{d}|\mathbf{p}_2| = E_2\,\mathrm{d}E_2\,. \tag{2.28}$$

Substituting $p_2^2 = m_2^2$, Eq. (2.21) and Eq. (2.28) into Eq. (2.26), one can show:

$$R_{1\to2}(s_1, m_2^2, m_3^2) = \frac{1}{(2\pi)^2}\int \frac{|\mathbf{p}_2|E_2\,\mathrm{d}E_2\,\mathrm{d}\cos\theta_{12}\,\mathrm{d}\phi_{12}}{2E_2}\delta(s_1 - 2\sqrt{s_1}E_2 + m_2^2 - m_3^2) \tag{2.29}$$

$$= \frac{1}{(2\pi)^2}\int \frac{|\mathbf{p}_2|\,\mathrm{d}\cos\theta_{12}\,\mathrm{d}\phi_{12}}{4\sqrt{s_1}}. \tag{2.30}$$

Eq. (2.30) gives a constraint of the energy E_2:

$$E_2 = \frac{s_1 + m_2^2 - m_3^2}{2\sqrt{s_1}}. \tag{2.31}$$

From the condition (2.27) and Eq. (2.31), the absolute value of $\mathbf{p}_2$ can be derived:

$$|\mathbf{p}_2| = (E_2^2 - m_2^2)^{1/2} \tag{2.32}$$

$$= \frac{\sqrt{(s_1 - m_2^2 - m_3^2)^2 - 4m_2^2m_3^2}}{2\sqrt{s_1}}. \tag{2.33}$$

Therefore, we can write the integration of 2-body phase space of the decay process as:

$$R_{1\to2}(s_1, m_2^2, m_3^2) = \frac{1}{(2\pi)^2}\int_{-1}^{1}\mathrm{d}\cos\theta_{12}\int_0^{2\pi}\mathrm{d}\phi_{12}\left[\frac{\lambda^{1/2}(s_1, m_2^2, m_3^2)}{8s_1}\right], \tag{2.34}$$

where $\lambda(a, b, c)$ is Källén function (or triangle function):

$$\lambda(a, b, c) = (a - b - c)^2 - 4bc. \tag{2.35}$$

2.1.2 Two-particle scattering

Considering the reaction $2 \to 2$:

$$p_1 + p_2 \to p_3 + p_4 \tag{2.36}$$

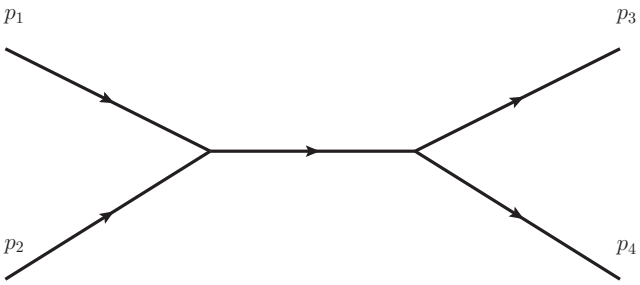

Figure 2.1: The 2 by 2 process

In the center of mass system (CMS), the total three-momentum of the incoming particles is zero and hence, the total three-momentum of the outgoing particles is $\mathbf{p}_3 + \mathbf{p}_4 = \mathbf{p}_1 + \mathbf{p}_2 = 0$. We have:

$$s_{12} \equiv (p_1 + p_2)^2 = (p_3 + p_4)^2 \tag{2.37}$$
$$= (E_1 + E_2)^2 = (E_3 + E_4)^2. \tag{2.38}$$

Using Eq. (2.5), the two-particle phase space integral can be obtained:

$$R_{2\to2}(s_{12}, m_3^2, m_4^2) = \int (2\pi)^4 \delta^4(p_1 + p_2 - p_3 - p_4) \frac{\mathrm{d}^3\mathbf{p}_3}{(2\pi)^3 2E_3} \frac{\mathrm{d}^3\mathbf{p}_4}{(2\pi)^3 2E_4}. \tag{2.39}$$

The $2 \to 2$ integral phase space can be constructed in the similar procedure as shown in the Subsection 2.1.1:

$$R_{2\to2}(s_{12}, m_3^2, m_4^2) = \frac{1}{(2\pi)^2} \int_{-1}^{1} \mathrm{d}\cos\theta_{13} \int_0^{2\pi} \mathrm{d}\phi_{13} \left[\frac{\lambda^{1/2}(s_{12}, m_3^2, m_4^2)}{8 s_{12}} \right]. \tag{2.40}$$

where θ_{13} is the polar angle between $\mathbf{p}_3$ and $\mathbf{p}_1$, ϕ_{13} is azimuthal orientation of $\mathbf{p}_3$ around $\mathbf{p}_1$.

Another possible way to compute $R_{2\to2}$ is using the invariant momentum transfer t:

$$t \equiv (p_1 - p_3)^2$$
$$= m_1^2 + m_3^2 - 2p_1.p_3$$
$$= m_1^2 + m_3^2 - 2(E_1 E_3 - |\mathbf{p}_1||\mathbf{p}_3| \cos\theta_{13}) \tag{2.41}$$
$$\Rightarrow \mathrm{d}t = 2|\mathbf{p}_1||\mathbf{p}_3| \, \mathrm{d}\cos\theta_{13} \tag{2.42}$$
$$\Rightarrow \mathrm{d}\cos\theta_{13} = \frac{\mathrm{d}t}{2|\mathbf{p}_1||\mathbf{p}_3|}. \tag{2.43}$$

By using the fact that $2 \to 2$ scattering has a cylindrical symmetry, ϕ_{13} is a trivial variable. We can take the integration over ϕ_{13} and substitute Eq. (2.43) into Eq. (2.40).
$R_{2\to2}$ can be written as:

$$R_{2\to2}(s_{12}, m_3^2, m_4^2) = \frac{1}{16\pi |\mathbf{p}_1| \sqrt{s_{12}}} \int_{t^-}^{t^+} \mathrm{d}t \, . \tag{2.44}$$

From $\cos\theta_{13} = \pm 1$ and $|\mathbf{p}_1| = \lambda^{1/2}(s_{12}, m_1^2, m_2^2)/(2\sqrt{s_{12}})$, we can derive the constraint of t:

$$t^{\pm} = m_1^2 + m_3^2 - 2(E_1 E_3 \mp |\mathbf{p}_1||\mathbf{p}_3|). \tag{2.45}$$

2.2 Three-particle final states

Collision of $2 \to 3$ process:

$$p_1 + p_2 \to p_3 + p_4 + p_5 \tag{2.46}$$

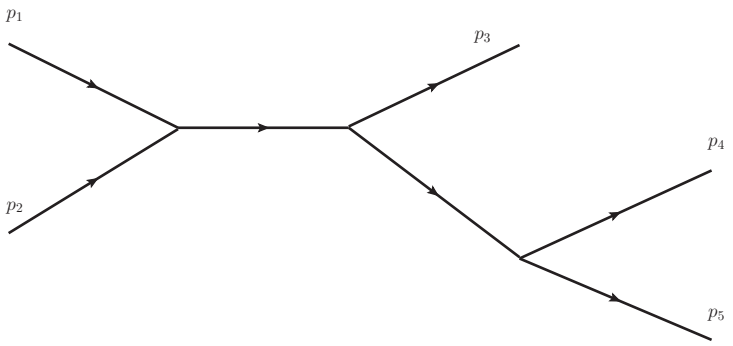

Figure 2.2: The $2 \to 3$ scattering decomposed into a $2 \to 2$ process and a $1 \to 2$ decay.

The integral of phase space is:

$$R_{2\to3}(s_{12}, m_3^2, m_4^2, m_5^2) = \int (2\pi)^4 \delta^4(p_1 + p_2 - p_3 - p_4 - p_5) \times \frac{\mathrm{d}^3\mathbf{p}_3}{(2\pi)^3 2E_3} \frac{\mathrm{d}^3\mathbf{p}_4}{(2\pi)^3 2E_4} \frac{\mathrm{d}^3\mathbf{p}_5}{(2\pi)^3 2E_5}. \tag{2.47}$$

To decompose the $2 \to 3$ into a $2 \to 2$ process and a $1 \to 2$ decay, we use this identity:

$$\begin{aligned} 1 &= \int \mathrm{d}s_{45} \int \frac{\mathrm{d}^3\mathbf{p}_{45}}{2E_{45}} \delta^4(p_{45} - p_4 - p_5) \\ &= \int \mathrm{d}s_{45} \int \mathrm{d}^4 p_{45}\, \delta(p_{45}^2 - s_{45}) \delta^4(p_{45} - p_4 - p_5) \\ &= \int \mathrm{d}s_{45}\, \delta((p_4 + p_5)^2 - s_{45}), \end{aligned} \tag{2.48}$$

where $E_{45}^2 = |\mathbf{p}_{45}|^2 + s_{45}$. We insert the identity (2.48) into Eq. (2.47) and get the result:

$$\begin{aligned} R_{2\to3}(s_{12}, m_3^2, m_4^2, m_5^2) = \frac{1}{2\pi} \int \mathrm{d}s_{45} \left\{ \int (2\pi)^4 \frac{\mathrm{d}^3\mathbf{p}_3}{(2\pi)^3 2E_3} \frac{\mathrm{d}^3\mathbf{p}_{45}}{(2\pi)^3 2E_{45}} \delta^4(p_1 + p_2 - p_3 - p_{45}) \right\} \\ \times \left\{ \int (2\pi)^4 \frac{\mathrm{d}^3\mathbf{p}_4}{(2\pi)^3 2E_4} \frac{\mathrm{d}^3\mathbf{p}_5}{(2\pi)^3 2E_5} \delta^4(p_{45} - p_4 - p_5) \right\}. \end{aligned} \tag{2.49}$$

The first bracket can be seen as a reaction of two particles in the CMS of $p_1 + p_2$ and the second is a decay process in the rest system (RS) of p_{45}. In concise form it is:

$$R_{2\to3}(s_{12}, m_3^2, m_4^2, m_5^2) = \frac{1}{2\pi} \int \mathrm{d}s_{45}\, R_{2\to2}(s_{12}, m_3^2, s_{45}) R_{1\to2}(s_{45}, m_4^2, m_5^2). \tag{2.50}$$

We choose the first term $R_{2\to2}$ by Eq. (2.40) and Eq. (2.34) for the second $R_{1\to2}$. We denote different frame by upper indices, $R12$ stand for CMS of $p_1 + p_2$ and $R45$ is the RS of p_{45}.

$$R_{2\to3}(s_{12},m_3^2,m_4^2,m_5^2)=\frac{1}{(2\pi)^5}\int \mathrm{d}s_{45}\int_{-1}^{1}\mathrm{d}\cos\theta^{R12}\int_0^{2\pi}\mathrm{d}\phi^{R12}\,\frac{\lambda^{1/2}(s_{12},m_3^2,s_{45})}{8s_{12}} \times\int_{-1}^{1}\mathrm{d}\cos\theta^{R45}\int_0^{2\pi}\mathrm{d}\phi^{R45}\,\frac{\lambda^{1/2}(s_{45},m_4^2,m_5^2)}{8s_{45}}, \quad (2.51)$$

in which:

$$s_{12}=(p_1+p_2)^2, \quad (2.52)$$
$$s_{45}=(p_4+p_5)^2. \quad (2.53)$$

The solid angle $\Omega^{R12}=(\theta^{R12},\phi^{R12})$ defines the orientations of $\mathbf{p}_3$ with respect to $\mathbf{p}_1$ in the $R12$ frame, and $\Omega^{R45}=(\theta^{R45},\phi^{R45})$ describes the orientations of $\mathbf{p}_4$ in the rest frame of p_{45}.

We shall next analyze the boundary region of the integral in the variable s_{45} in the $R12$ frame. Because of the on-shell condition $E_3^2=|\mathbf{p}_3|^2+m_3^2\geq m_3^2$, we have:

$$\begin{aligned}s_{45}=(p_4+p_5)^2&=(p_1+p_2-p_3)^2=s_{12}-2\sqrt{s_{12}}E_3+p_3^2\\&=s_{12}-2\sqrt{s_{12}}E_3+m_3^2\leq s_{12}-2\sqrt{s_{12}}m_3+m_3^2,\end{aligned} \quad (2.54)$$

i.e.

$$s_{45}\leq(\sqrt{s_{12}}-m_3)^2, \quad (2.55)$$

and in the $R45$ frame:

$$s_{45}=(E_4+E_5)^2\geq(m_4+m_5)^2, \quad (2.56)$$

give the constraint of s_{45}:

$$(m_4+m_5)^2\leq s_{45}\leq(\sqrt{s_{12}}-m_3)^2. \quad (2.57)$$

2.3 Total cross-section

We now establish the analytical formula of the total cross-section in a $2\to3$ scattering:

$$\sigma_{2\to3}=\frac{1}{Z}\int(2\pi)^4|\mathcal{M}|^2\delta^4(p_1+p_2-p_3-p_4-p_5) \times\frac{\mathrm{d}^3\mathbf{p}_3}{(2\pi)^3 2E_3}\frac{\mathrm{d}^3\mathbf{p}_4}{(2\pi)^3 2E_4}\frac{\mathrm{d}^3\mathbf{p}_5}{(2\pi)^3 2E_5}, \quad (2.58)$$

where

$$\begin{aligned}Z&=4\sqrt{(p_1.p_2)^2-m_1^2m_2^2}\\&=4\sqrt{\frac{(s_{12}-m_1^2-m_2^2)^2}{4}-m_1^2m_2^2}\\&=4\sqrt{\frac{(s_{12}-m_1^2-m_2^2)^2-4m_1^2m_2^2}{4}\times\frac{s_{12}}{s_{12}}}\\&=4\frac{\lambda^{1/2}(s_{12},m_1^2,m_2^2)}{2\sqrt{s_{12}}}\sqrt{s_{12}}\\&=4|\mathbf{p}_1|\sqrt{s_{12}}.\end{aligned} \quad (2.59)$$

From Eq. (2.51), Eq. (2.57) and Eq. (2.59), we obtain:

$$\sigma_{2\to3} = \frac{1}{4(2\pi)^5|\mathbf{p}_1|\sqrt{s_{12}}}\int_{(m_4+m_5)^2}^{(\sqrt{s_{12}}-m_3)^2} \mathrm{d}s_{45} \times\left[\int_{-1}^{1}\mathrm{d}\cos\theta^{R12}\int_0^{2\pi}\mathrm{d}\phi^{R12}\,\frac{\lambda^{1/2}(s_{12},m_3^2,s_{45})}{8s_{12}}\right] \times\left[\int_{-1}^{1}\mathrm{d}\cos\theta^{R45}\int_0^{2\pi}\mathrm{d}\phi^{R45}\,\frac{\lambda^{1/2}(s_{45},m_4^2,m_5^2)}{8s_{45}}\right]|\mathcal{M}(p_i)|^2, \quad (2.60)$$

where p_i is the momenta in one frame.
From this we define the phase space volume:

$$V_{PS} = \int_{(m_4+m_5)^2}^{(\sqrt{s_{12}}-m_3)^2}\mathrm{d}s_{45}\,\frac{\lambda^{1/2}(s_{12},m_3^2,s_{45})\lambda^{1/2}(s_{45},m_4^2,m_5^2)}{512\pi^3|\mathbf{p}_1|s_{45}(s_{12})^{3/2}}. \quad (2.61)$$

In Eq. (2.60), the total cross-section is written in terms of invariant variables s_{12}, s_{45}. The geometric variables (ϕ^{R12}, θ^{R12}, ϕ^{R45}, θ^{R45}) are computed in different reference frames. However, to calculate $|\mathcal{M}|^2$ we need to have all momenta in one reference frame. This is a remaining problem that we will solve in the next section.

2.4 Generating set of momentum

The main technique to calculate the total cross-section numerically is generating the set of momentum configurations in one reference frame. However, in Eq. (2.60) remains two different frames $R12$ and $R45$. So, this section is organized to transform all kinematical variables into the CMS of $p_1 + p_2$ via Lorentz transformation tools which well-known formulas can be found in Appendix B. We step by step construct the individual set of momenta in the specific frames (R^{12} and R^{45}) and combine them at the end of the section, respectively:
R^{12} and R^{45} correspond to:

- CMS of process $p_1 + p_2 \to p_3 + p_{45}$,
- Rest frame of process $p'_{45} \to p'_4 + p'_5$.

The four-momentum $p_i(i = 1, 2, 3, 45)$ and $p'_j(j = 45, 4, 5)$ will be parameterized with the space components being written in the three-dimensional spherical coordinates. We also relabel (θ^{R12}, ϕ^{R12}) in $R12$ frame to (θ_{13}, ϕ_{13}) and similarly (θ^{R45}, ϕ^{R45}) to (θ_{45}, ϕ_{45}). All kinematical variables of particles in R^{12} and R^{45} frame can be written in terms of the four-vectors which is convenient for numerical calculation. Especially in the R^{12} frame:

$$p_1 = (E_1, \mathbf{p}_1) = (E_1, 0, 0, |\mathbf{p}_1|), \quad (2.62)$$
$$p_2 = (E_2, \mathbf{p}_2) = (E_2, 0, 0, -|\mathbf{p}_1|), \quad (2.63)$$
$$p_3 = (E_3, \mathbf{p}_3) = (E_3, |\mathbf{p}_3|\sin(\theta_{13})\sin(\phi_{13}), |\mathbf{p}_3|\sin(\theta_{13})\cos(\phi_{13}), |\mathbf{p}_3|\cos(\theta_{13})), \quad (2.64)$$
$$p_{45} = (E_{45}, \mathbf{p}_{45}) = (E_{45}, -|\mathbf{p}_3|\sin(\theta_{13})\sin(\phi_{13}), -|\mathbf{p}_3|\sin(\theta_{13})\cos(\phi_{13}), -|\mathbf{p}_3|\cos(\theta_{13})). \quad (2.65)$$

From Eq. (2.62) to Eq. (2.65), we get:

$$E_1 = \frac{s_{12} + m_1^2 - m_2^2}{2\sqrt{s_{12}}}, \tag{2.66}$$

$$E_2 = \sqrt{s_{12}} - E_1, \tag{2.67}$$

$$|\mathbf{p}_1| = \frac{\lambda^{1/2}(s_{12}, m_1^2, m_2^2)}{2\sqrt{s_{12}}}, \tag{2.68}$$

$$E_3 = \frac{s_{12} + m_3^2 - s_{45}}{2\sqrt{s_{12}}}, \tag{2.69}$$

$$E_{45} = \sqrt{s_{12}} - E_3, \tag{2.70}$$

$$|\mathbf{p}_3| = \frac{\lambda^{1/2}(s_{12}, m_3^2, s_{45})}{2\sqrt{s_{12}}}. \tag{2.71}$$

Similarly, in the rest frame of p'_{45}, the set of momenta is:

$$p'_{45} = (E'_{45}, \mathbf{p}'_{45}) = (E'_{45}, 0, 0, 0) = (\sqrt{s_{45}}, 0, 0, 0), \tag{2.72}$$

$$p'_4 = (E'_4, \mathbf{p}'_4) = (E'_4, |\mathbf{p}'_4|\sin(\theta_{45})\sin(\phi_{45}), |\mathbf{p}'_4|\sin(\theta_{45})\cos(\phi_{45}), |\mathbf{p}'_4|\cos(\theta_{45})), \tag{2.73}$$

$$\begin{aligned} p'_5 &= (E'_5, \mathbf{p}'_5) \\ &= (E'_5, -|\mathbf{p}'_4|\sin(\theta_{45})\sin(\phi_{45}), -|\mathbf{p}'_4|\sin(\theta_{45})\cos(\phi_{45}), -|\mathbf{p}'_4|\cos(\theta_{45})). \end{aligned} \tag{2.74}$$

where:

$$|\mathbf{p}'_4| = \frac{\lambda^{1/2}(s_{45}, m_4^2, m_5^2)}{2\sqrt{s_{45}}}, \tag{2.75}$$

$$E'_4 = \frac{s_{45} + m_4^2 - m_5^2}{2\sqrt{s_{45}}}, \tag{2.76}$$

$$E'_5 = \sqrt{s_{45}} - E'_4. \tag{2.77}$$

For the previous requirement that the total cross-section must be computed in the CMS of $p_1 + p_2$. We then transform the p'_4 and p'_5 from R^{45} frame to R^{12} frame. p_{45} and p'_{45} can be used to obtain the relative velocity of the two frames. Because the velocity of p'_{45} in $R45$ is zero, then the relative velocity is the velocity of p_{45} in the CMS of $p_1 + p_2$:

$$\mathbf{v}_{45} = \frac{\mathbf{p}_{45}}{E_{45}}. \tag{2.78}$$

Inserting $\mathbf{v}_{45}$ in Eq. (2.78) into a Lorentz boost matrix in Eq. (B.17) (Appendix B). We obtain $p_4 = (E_4, \mathbf{p}_4)$ and $p_5 = (E_5, \mathbf{p}_5)$ in the CMS of $p_1 + p_2$. We can now use the $(p_1,\ p_2,\ p_3,\ p_4,\ p_5)$ to compute the $|\mathcal{M}|^2$.

CHAPTER

THREE

BREMSSTRAHLUNG PROCESS $e\mu \to e\mu\gamma$ IN QED

In experiment, we measure the cross-section of the process $e\mu \to e\mu + N\gamma$ where $N = 0, 1, 2, \ldots, \infty$.
In the LO approximation, we take $N = 0$ and $\sigma = \sigma_{\rm LO} = \sigma_0(e\mu \to e\mu) \sim \mathcal{O}(\alpha^2)$.
In the NLO approximation, we have $N = 0, 1$ and
$\sigma = \sigma_{\rm LO} + \sigma_0(e\mu \to e\mu + \gamma) + \sigma_{\rm virt}(e\mu \to e\mu)$, where:

$$\sigma_0(e\mu \to e\mu + \gamma) = \sigma_{\rm soft}(E_\gamma < \Delta E) + \sigma_{\rm hard}(E_\gamma > \Delta E). \tag{3.1}$$

Our work is computing the cross-section $\sigma_{\rm hard}$ of the bremsstrahlung process
$e\mu \to e\mu + \gamma$ which is the hard-photon corrections. Combining this result with the soft-photon corrections and the virtual-corrections in Le Duc Truyen's thesis Ref. [6] gives the NLO QED corrections to the $e\mu \to e\mu$ scattering. At the end of this chapter, we prove the cross-section at the NLO is independent of a parameter ΔE.

$$\sigma_{\rm NLO}^{\rm QED} = \sigma_{\rm LO} + \sigma_{\rm virt} + \sigma_{\rm real}(\alpha^3), \tag{3.2}$$

where

$$\sigma_{\rm real}(\alpha^3) = \sigma_{\rm soft}(\alpha^3, \Delta E) + \sigma_{\rm hard}(\alpha^3, \Delta E). \tag{3.3}$$

3.1 Feynman Amplitude

Consider the Bremsstrahlung scattering process:

$$e(p_1) + \mu(p_2) \to e(p_3) + \mu(p_4) + \gamma(k) \tag{3.4}$$

There is four possible photon emission process that can exist corresponding to four Feynman diagrams. Based on the Feynman rules in Section 1.2, we can write down the Feynman amplitudes of process (3.4) using the Feynman diagrams Fig. 3.1 - Fig. 3.4. The arrow on each external line which is the fermion flow coincides with the momentum direction. For an external photon, photon propagator, and internal fermion the momentum direction was denoted by the arrow line next to it.

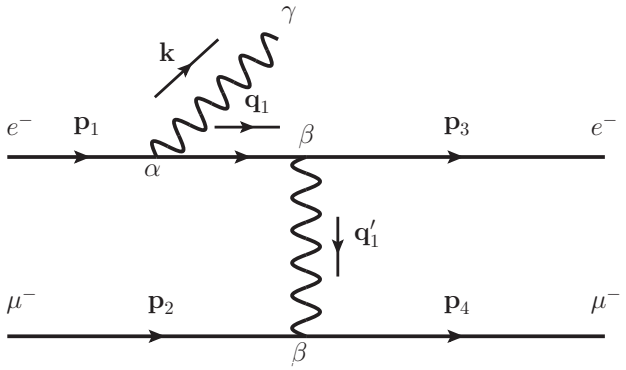

Figure 3.1: The photon emission off the incoming electron

In Fig. 3.1, we have the Feynman Amplitude:

$$\mathcal{M}_1 = ie^3 \frac{1}{[(p_1-k)^2 - m_e^2](p_2-p_4)^2} \times \bar{u}^{s_3}(p_3)\gamma^\beta(\not{p}_1 - \not{k} + m_e)\gamma^\alpha u^{s_1}(p_1)\bar{u}^{s_4}(p_4)\gamma_\beta u^{s_2}(p_2)\epsilon^*_\alpha(k).$$

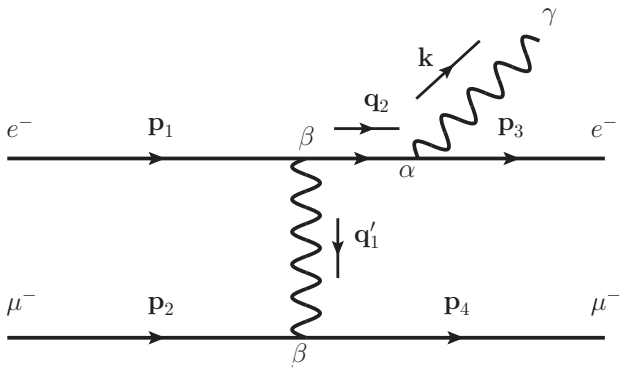

Figure 3.2: The photon emission off the outgoing electron

In Fig. 3.2, we have the Feynman Amplitude:

$$\mathcal{M}_2 = ie^3 \frac{1}{[(p_3+k)^2 - m_e^2](p_2-p_4)^2} \times \bar{u}^{s_3}(p_3)\gamma^\alpha(\not{p}_3 + \not{k} + m_e)\gamma^\beta u^{s_1}(p_1)\bar{u}^{s_4}(p_4)\gamma_\beta u^{s_2}(p_2)\epsilon^*_\alpha(k).$$

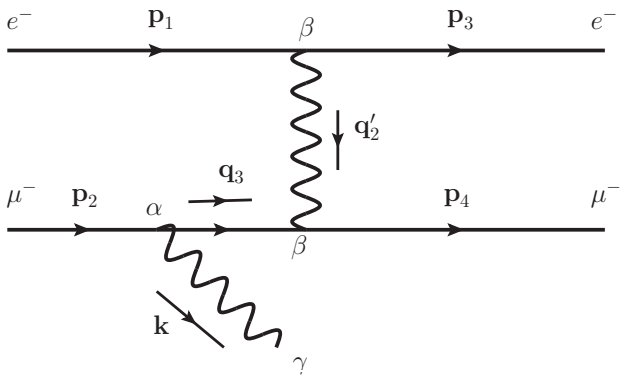

Figure 3.3: The photon emission off the incoming muon

In Fig. 3.3, we have the Feynman Amplitude:

$$\mathcal{M}_3 = ie^3 \frac{1}{\left[(p_2-k)^2 - m_\mu^2\right](p_1-p_3)^2} \times \bar{u}^{s_4}(p_4)\gamma^\beta(\not{p}_2 - \not{k} + m_\mu)\gamma^\alpha u^{s_2}(p_2)\bar{u}^{s_3}(p_3)\gamma_\beta u^{s_1}(p_1)\epsilon_\alpha^*(k).$$

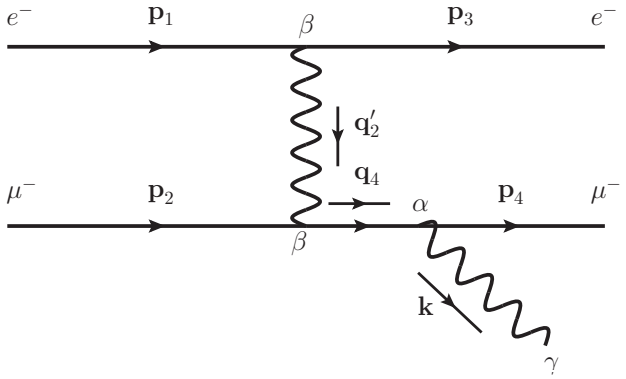

Figure 3.4: The photon emission off the outgoing muon

In Fig. 3.4, we have the Feynman Amplitude:

$$\mathcal{M}_4 = ie^3 \frac{1}{\left[(p_4+k)^2 - m_\mu^2\right](p_1-p_3)^2} \times \bar{u}^{s_4}(p_4)\gamma^\alpha(\not{p}_4 + \not{k} + m_\mu)\gamma^\beta u^{s_2}(p_2)\bar{u}^{s_3}(p_3)\gamma_\beta u^{s_1}(p_1)\epsilon_\alpha^*(k).$$

In case of unpolarized beams, we do not know the spin of the initial particles. Thus, we have to average overall all spin states by including the overall factor $\frac{1}{4}$ in the squared amplitude:

$$|\mathcal{M}|^2 = \frac{1}{4}\sum_{s_1,s_2,s_3,s_4} |\mathcal{M}_1 + \mathcal{M}_2 + \mathcal{M}_3 + \mathcal{M}_4|^2. \tag{3.5}$$

The expression of the amplitude squared is too long to display here. It is automatically calculated with the help of the symbolic manipulation program Form [13]. The reader can find this code in the Appendix C.0.3

3.2 Phase space mappings in the numerical integration

Mapping is the specific combination of the final particles into a subset, aiming to use the Lorentz transformation to breakdown the multi-particles final state in $2 \to n$ scattering to sub-processes $2 \to 2$ and $1 \to 2$. For instance, in Section 2.4, the muon and photon in the final state are combined. Then, we will call them as the mapping (45)3. Because our scattering has three final particles state then there are three possible ways to combine them into three mappings.

- Mapping (45)3 is a combination of the final state of electron and photon,
- Mapping (35)4 is a combination of the final state of electron and photon,
- Mapping (34)5 is a combination of the final state of electron and muon.

Mapping illustrates the different sets of momenta. It is not only cross-checked against the numerical results of an observable quantity in the certain scattering process but also the improving efficient convergence rate if we find out the best mapping.

3.2.1 Mapping (45)3

Mapping (45)3 has already been constructed in Section 2.3 where the formula of the cross-section Eq. (2.60) and the set of kinematical variables have been provided. Besides, the set of momenta in the $R12$ frame has been established in Section 2.4.

3.2.2 Mapping (35)4

The total cross-section of $e\mu \to e\mu\gamma$ scattering based on Eq. (2.58) is:

$$\sigma = \frac{1}{Z}\int (2\pi)^4 |\mathcal{M}|^2 \delta^4(p_1 + p_2 - p_3 - p_4 - k) \frac{\mathrm{d}^3\mathbf{p}_3}{(2\pi)^3 2E_3} \frac{\mathrm{d}^3\mathbf{p}_4}{(2\pi)^3 2E_4} \frac{\mathrm{d}^3\mathbf{k}}{(2\pi)^3 2k_0}. \tag{3.6}$$

Using the familiar identity to decompose the $2 \to 3$ process into two parts by:

$$1 = \int \mathrm{d}s_{35} \int \frac{\mathrm{d}^3\mathbf{p}_{35}}{2E_{35}} \delta^4(p_{35} - p_3 - k), \tag{3.7}$$

where

$$s_{35} = (p_3 + k)^2. \tag{3.8}$$

We take the similar procedure to obtain the total cross-section in Section 2.3 and Eq. (2.59). Then, we can derive the total cross-section σ in the mapping (35)4 as:

$$\begin{aligned}\sigma = \frac{1}{4(2\pi)^5 |\mathbf{p}_1| \sqrt{s_{12}}} \int_{m_e^2}^{(\sqrt{s_{12}} - m_\mu)^2} \mathrm{d}s_{35} \left[\int_{-1}^{1} \mathrm{d}\cos\theta_{14} \int_0^{2\pi} \mathrm{d}\phi_{14} \frac{\lambda^{1/2}(s_{12}, m_\mu^2, s_{35})}{8 s_{12}} \right] \\ \times \left[\int_{-1}^{1} \mathrm{d}\cos\theta_{35} \int_0^{2\pi} \mathrm{d}\phi_{35} \frac{\lambda^{1/2}(s_{35}, m_e^2, m_k^2)}{8 s_{35}} \right] |\mathcal{M}|^2,\end{aligned} \tag{3.9}$$

where $\Omega^{14} = (\cos\theta_{14}, \phi_{14})$ is the solid angle describing the orientation of $\mathbf{p}_4$ with respect to $\mathbf{p}_1$ in the CMS of process $p_1 + p_2 \to p_4 + p_{35}$ and $\Omega^{35} = (\cos\theta_{35}, \phi_{35})$ describes the orientation of $\mathbf{p}_3$ in the rest frame of process $p'_{35} \to p'_3 + k'$.

According to the procedure of generating the set of momenta in Section 2.4, we now construct the formulas to compute energies and momenta in mapping (34)5.
The value of the total energy and momentum of the incoming muon and the electron are obtained from Eq. (2.66) to Eq. (2.68) by replacing (m_1, m_2) into (m_e, m_μ), respectively. In the CMS of process $p_1 + p_2 \to p_4 + p_{35}$:

$$|\mathbf{p}_4| = \frac{\lambda^{1/2}(s_{12}, m_\mu^2, s_{35})}{2\sqrt{s_{12}}}, \tag{3.10}$$

$$E_4 = \frac{s_{12} + m_\mu^2 - s_{35}}{2\sqrt{s_{12}}}, \tag{3.11}$$

$$E_{35} = \sqrt{s_{12}} - E_4. \tag{3.12}$$

So, the set of momenta is:

$$p_1 = (E_1, \mathbf{p}_1) = (E_1, 0, 0, |\mathbf{p}_1|), \tag{3.13}$$

$$p_2 = (E_2, \mathbf{p}_2) = (E_2, 0, 0, -|\mathbf{p}_1|), \tag{3.14}$$

$$p_4 = (E_4, \mathbf{p}_4) = (E_4, |\mathbf{p}_4|\sin(\theta_{14})\sin(\phi_{14}), |\mathbf{p}_4|\sin(\theta_{14})\cos(\phi_{14}), |\mathbf{p}_4|\cos(\theta_{14})), \tag{3.15}$$

$$\begin{aligned} p_{35} &= (E_{35}, \mathbf{p}_{35}) \\ &= (E_{35}, -|\mathbf{p}_4|\sin(\theta_{14})\sin(\phi_{14}), -|\mathbf{p}_4|\sin(\theta_{14})\cos(\phi_{14}), -|\mathbf{p}_4|\cos(\theta_{14})). \end{aligned} \tag{3.16}$$

In the rest frame of p'_{35}, the energy and momentum is:

$$|\mathbf{p}'_3| = \frac{\lambda^{1/2}(s_{35}, m_e^2, m_k^2)}{2\sqrt{s_{35}}}, \tag{3.17}$$

$$E'_3 = \frac{s_{35} + m_e^2 - m_k^2}{2\sqrt{s_{35}}}, \tag{3.18}$$

$$k'_0 = \sqrt{s_{35}} - E'_3. \tag{3.19}$$

The set of momenta is:

$$p'_{35} = (E'_{35}, \mathbf{p}'_{35}) = (E'_{35}, 0, 0, 0) = (\sqrt{s_{35}}, 0, 0, 0), \tag{3.20}$$

$$p'_3 = (E'_3, \mathbf{p}'_3) = (E'_3, |\mathbf{p}'_3|\sin(\theta_{35})\sin(\phi_{35}), |\mathbf{p}'_3|\sin(\theta_{35})\cos(\phi_{35}), |\mathbf{p}'_3|\cos(\theta_{35})), \tag{3.21}$$

$$\begin{aligned} k' &= (k'_0, \mathbf{k}') \\ &= (k'_0, -|\mathbf{p}'_3|\sin(\theta_{35})\sin(\phi_{35}), -|\mathbf{p}'_3|\sin(\theta_{35})\cos(\phi_{35}), -|\mathbf{p}'_3|\cos(\theta_{35})). \end{aligned} \tag{3.22}$$

Then we transform the p'_3 and k' into the CMS of $p_1 + p_2$ by the Lorentz transformation in the similar fashion in Section 2.4.

3.2.3 Mapping (34)5

In the mapping (34)5 we define the invariant mass squared as:

$$s_{34} = (p_3 + p_4)^2. \tag{3.23}$$

And the solid angle $\Omega^{15} = (\cos\theta_{15}, \phi_{15})$ present the orientation of $\mathbf{k}$ around a beam axis $\mathbf{p}_1$ in the CMS frame of $p_1 + p_2 \to k + p_{34}$ and $\Omega^{34} = (\cos\theta_{34}, \phi_{34})$ is the solid angle of orientation of $\mathbf{p}'_3$ in the rest frame of process $p'_{34} \to p'_3 + p'_4$.
The total cross-section in the mapping (34)5 is:

$$\sigma = \frac{1}{4(2\pi)^5 |\mathbf{p}_1|\sqrt{s_{12}}} \int_{(m_e+m_\mu)^2}^{s_{12}} \mathrm{d}s_{34} \left[\int_{-1}^{1} \mathrm{d}\cos\theta_{15} \int_0^{2\pi} \mathrm{d}\phi_{15} \, \frac{\lambda^{1/2}(s_{12}, m_k^2, s_{34})}{8 s_{12}} \right] \times \left[\int_{-1}^{1} \mathrm{d}\cos\theta_{34} \int_0^{2\pi} \mathrm{d}\phi_{34} \, \frac{\lambda^{1/2}(s_{34}, m_e^2, m_\mu^2)}{8 s_{34}} \right] |\mathcal{M}|^2. \tag{3.24}$$

From the similar procedure in Subsection 3.2.2, we have the following formulas of energy and momentum of particles in two reference frames (R12 and R34) and the set of momenta. In the CMS of $p_1 + p_2 \to k + p_{34}$:

$$|\mathbf{k}| = \frac{\lambda^{1/2}(s_{12}, m_k^2, s_{34})}{2\sqrt{s_{12}}}, \tag{3.25}$$

$$k_0 = \frac{s_{12} + m_k^2 - s_{34}}{2\sqrt{s_{12}}}, \tag{3.26}$$

$$E_{34} = \sqrt{s_{12}} - k_0. \tag{3.27}$$

The set of momenta is given by:

$$p_1 = (E_1, \mathbf{p}_1) = (E_1, 0, 0, |\mathbf{p}_1|), \tag{3.28}$$

$$p_2 = (E_2, \mathbf{p}_2) = (E_2, 0, 0, -|\mathbf{p}_1|), \tag{3.29}$$

$$k = (k_0, \mathbf{k}) = (k_0, |\mathbf{k}|\sin(\theta_{15})\sin(\phi_{15}), |\mathbf{k}|\sin(\theta_{15})\cos(\phi_{15}), |\mathbf{k}|\cos(\theta_{15})), \tag{3.30}$$

$$\begin{aligned} p_{34} &= (E_{34}, \mathbf{p}_{34}) \\ &= (E_{34}, -|\mathbf{k}|\sin(\theta_{15})\sin(\phi_{15}), -|\mathbf{k}|\sin(\theta_{15})\cos(\phi_{15}), -|\mathbf{k}|\cos(\theta_{15})). \end{aligned} \tag{3.31}$$

In the rest frame of p'_{34} of process $p'_{34} \to p'_3 + p'_4$:

$$|\mathbf{p}'_3| = \frac{\lambda^{1/2}(s_{34}, m_e^2, m_\mu^2)}{2\sqrt{s_{34}}}, \tag{3.32}$$

$$E'_3 = \frac{s_{34} + m_e^2 - m_\mu^2}{2\sqrt{s_{34}}}, \tag{3.33}$$

$$E'_4 = \sqrt{s_{34}} - E'_3. \tag{3.34}$$

The set of momenta is:

$$p'_{34} = (E'_{34}, \mathbf{p}'_{34}) = (E'_{34}, 0, 0, 0) = (\sqrt{s_{34}}, 0, 0, 0), \tag{3.35}$$

$$p'_3 = (E'_3, \mathbf{p}'_3) = (E'_3, |\mathbf{p}'_3|\sin(\theta_{34})\sin(\phi_{34}), |\mathbf{p}'_3|\sin(\theta_{34})\cos(\phi_{34}), |\mathbf{p}'_3|\cos(\theta_{34})), \tag{3.36}$$

$$\begin{aligned} p'_4 &= (E'_4, \mathbf{p}'_4) \\ &= (E'_4, -|\mathbf{p}'_3|\sin(\theta_{34})\sin(\phi_{34}), -|\mathbf{p}'_3|\sin(\theta_{34})\cos(\phi_{34}), -|\mathbf{p}'_3|\cos(\theta_{34})). \end{aligned} \tag{3.37}$$

Finally, the analogous work in transformation p'_3 and p'_4 into the CMS of $p_1 + p_2$ follows as in Section 2.4.

3.3 Numerical Results

From the formula of the total cross-section that we have constructed in the previous section. We see that there are two important parts: the matrix element squared and the phase space integral. Before calculating the cross-section via BASES and VEGAS+, we check the amplitude squared between different programs. Next, we compute the cross-section with two cut-off conditions $\Delta E > 10^{-4}\sqrt{s}/2$ [GeV] and $E_3 > 0.2$ [GeV] in the lab frame in order to find the best phase space mapping. Finally, we present final results for the cross-section with applied cut $E_3 > 0.2$ [GeV] in the lab frame and $\Delta E > 10^{\mathrm{n}}\sqrt{s}/2$ [GeV] (n = -2,-3,...,-6).

3.3.1 Data set

We use the same following parameters in BASES and VEGAS+:

- Mass of electron $m_e = 0.1056583715$ [GeV],
- Mass of muon $m_\mu = 0.510998928 \times 10^{-3}$ [GeV],
- Mass of photon $m_k = 0$ [GeV],
- Constant k = 389.3793721 [GeV^{-2} μb] for converting from GEV^{-2} to μb,
- Fine structure constant $\alpha = 1/137.03599907430637$,
- The energy of the incoming Muon in lab frame E = 150 [GeV],
- Using s $= m_\mu^2 + m_e^2 + 2m_eE$ [GeV^{-2}] we get the colliding energy in the CMS:

$$E_{\mathrm{CMS}} = \sqrt{s} = 0.4055411581922807 \text{ [GeV]}.$$

3.3.2 Pre-Calculating

First, we check BASES and VEGAS+ at one phase space point in order to investigate the accuracy of the square of amplitude with the set of momenta (the unit is GeV) given by:

$$\begin{aligned}
p_1 &= (0.1890069571768645, 0.0, 0.0, 0.1890062664076317);\\
p_2 &= (0.2165342010154162, 0.0, 0.0, -0.1890062664076317);\\
p_3 &= (7.1653021113101970 \times 10^{-2}, -3.1654810669732455 \times 10^{-2},\\
&\quad -6.3710439572897432 \times 10^{-2}, -8.5350551036181589 \times 10^{-3});\\
p_4 &= (0.19453505093343165, 1.5691325908940491 \times 10^{-2},\\
&\quad 0.10599426903523390, -0.12328500231798974);\\
k &= (0.13935308614574704, 1.5963484760791957 \times 10^{-2},\\
&\quad -4.2283829462336477 \times 10^{-2}, 0.13182005742160791).
\end{aligned}$$

Table 3.1: Comparison of $|\mathcal{M}|^2$ (the average factor 1/4 is included) between BASES, VEGAS+ and FormCalc at one phase space point.

Feynman Amplitude Squared	
BASES	554.99751645972185
VEGAS+	554.99751645972481
FormCalc	554.997516459736

BASES and VEGAS+ use the squared amplitude produced by the FORM code in Appendix C.0.3. FormCalc [14] generates the squared amplitude automatically using the FeynArts [15]. The FormCalc result is provided by Dr. Le Duc Ninh.

We now introduce the definition of variation (VA) and relative error (RE) which help to further comprehend not only the precision of numerical results but also comparison of different calculations.
If two observables have the numerical representation $K_1 = \overline{K}_1 + \epsilon_1$ and $K_2 = \overline{K}_2 + \epsilon_2$. In which $\overline{K}_i (i = 1, 2)$ are the mean values and ϵ_i are the absolute errors. The VA between K_1 and K_2 is obtained by the relation:

$$\text{VA} = \frac{\left|\overline{K}_1 - \overline{K}_2\right|}{\sqrt{\epsilon_1^2 + \epsilon_2^2}} \text{ [sigma]}. \tag{3.38}$$

If VA ≤ 2 then we say that the two results agree well.
An individual measurement has the result $K = \overline{K} + \epsilon$. The RE is defined as:

$$\text{RE} = \frac{\epsilon \times 100}{\overline{K}} \text{ [\%]}. \tag{3.39}$$

The RE is a measure of precision. It presents how accurate a measurement is compared to the true value. The RE often write in the part per million (ppm) unit:

$$\text{RE} = \frac{\epsilon \times 10^6}{\overline{K}} \text{ [ppm]}. \tag{3.40}$$

Second, we compute the cross-section to check generating the set of momenta. We use the following conditions:

- The energy of the emission photon $\Delta E > 10^{-4}\sqrt{s}/2$ [GeV],
- The energy of the outgoing electron $E_3 > 0.2$ [GeV] in lab frame.

Table 3.2: Comparison the cross-section in the hard-photon region between BASES and VEGAS+ at the same 10^7 points. The VA is computed with respect to the mapping (34)5.

	Mapping (34)5	Mapping (35)4	Mapping (45)3
BASES	388.73(24)	387.74(80)	388.46(89)
RE [%]	0.0678	0.2067	0.2303
VA [sigma]	0	1.1882	0.2874
VEGAS+	388.653(35)	388.27(14)	388.61(15)
RE [%]	0.0090	0.0361	0.0386
VA [sigma]	0	2.6540	0.2792

Based on computing the cross-section in the hard-photon region, we find that the mapping (34)5 has the lowest RE not only in the VEGAS+ but also in the BASES.

3.3.3 Main result

Finally, we use the cut-off condition in the hard-photon region and the energy of the outgoing electron in lab frame:

- The energy of the emission photon $\Delta E > 10^{\mathrm{n}}\sqrt{s}/2$ [GeV] (n $= -2, -3, \ldots, -6$),
- The energy of the outgoing electron $E_3 > 0.2$ [GeV] in lab frame.

The cross-section at NLO is obtained by Eq. (3.2):

$$\sigma_{\mathrm{NLO}}^{\mathrm{QED}} = \sigma_{\mathrm{LO}} + \sigma_{\mathrm{virt}} + \sigma_{\mathrm{soft}}(\alpha^3, \Delta E) + \sigma_{\mathrm{hard}}(\alpha^3, \Delta E), \tag{3.41}$$

where the cross-section at LO (using Mathematica):

$$\sigma_{\mathrm{LO}} = 1265.0603541 \ [\mu\mathrm{b}]. \tag{3.42}$$

Table 3.3: Summary of the cross-section of the hard-photon corrections σ_{hard} [μb] by VEGAS+ using the mapping (34)5; the cross-section of the virtual and soft-photon corrections $\sigma_{\mathrm{virt\,+\,soft}}$ [μb] and the cross-section at NLO QED corrections $\sigma_{\mathrm{NLO}}^{\mathrm{QED}}$ [μb] at different n.

n	σ_{hard} [μb]	$\sigma_{\mathrm{virt\,+\,soft}}$ [μb]	$\sigma_{\mathrm{NLO}}^{\mathrm{QED}}$ [μb]	RE $\sigma_{\mathrm{NLO}}^{\mathrm{QED}}$ [ppm]
-2	209.1694(24)	-138.5914(16)	1335.6384(29)	2.17
-3	298.7590(36)	-228.5453(26)	1335.2741(44)	3.30
-4	388.6780(49)	-318.4989(37)	1335.2395(61)	4.57
-5	478.6436(66)	-408.4527(47)	1335.2513(81)	6.07
-6	568.6031(77)	-498.4066(57)	1335.2569(96)	7.19

Then, we calculate the relative corrections of the cross-section at the NLO (considering n = -4 in Table 3.3) to the cross-section of $e\mu \to e\mu$ scattering:

$$\delta_{\mathrm{NLO}} = \frac{\sigma_{\mathrm{NLO}}^{\mathrm{QED}} - \sigma_{\mathrm{LO}}}{\sigma_{\mathrm{LO}}} \times 100 \ [\%] \tag{3.43}$$

$$= \frac{1335.2394 - 1265.0603}{1265.0603} \times 100 \approx 5.5475 \ [\%]. \tag{3.44}$$

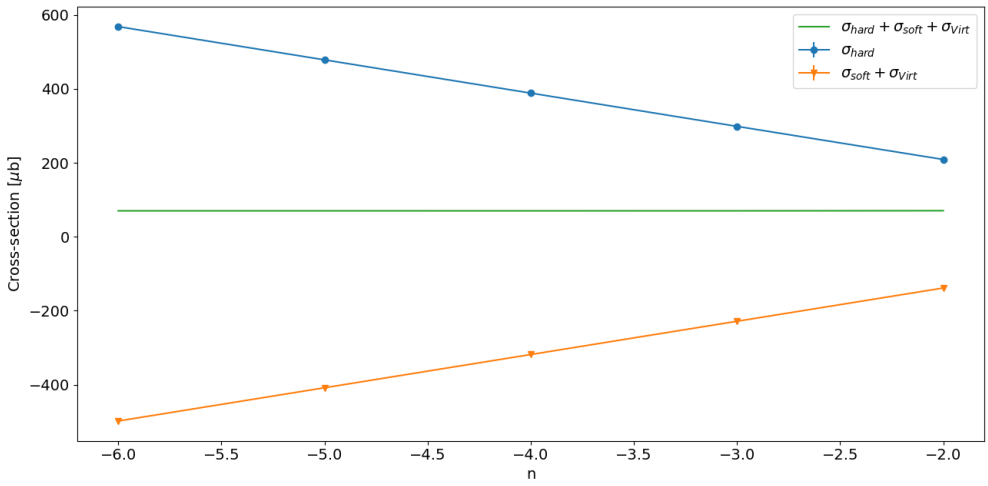

Figure 3.5: Dependence of the cross-section with respect to the parameter n which relates to the energy of the photon $\Delta E = 10^n\sqrt{s}/2$ [GeV].

In Fig. 3.5, the sum of the cross-section σ_{hard} and $\sigma_{\text{virt + soft}}$ is independent of ΔE. This result is consistent with our expectation.

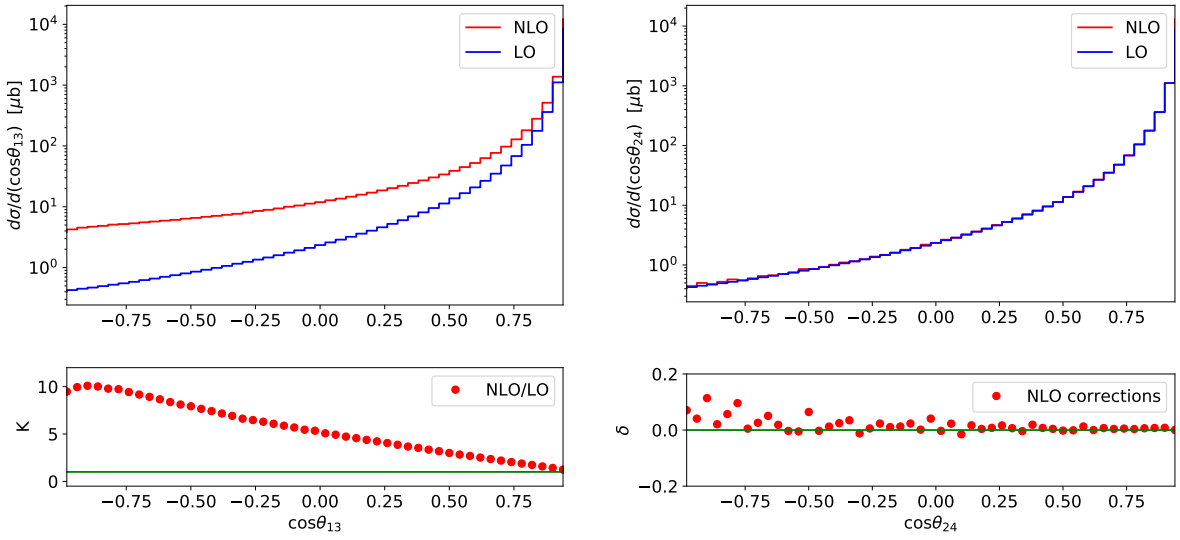

Figure 3.6: The LO and NLO QED differential cross-sections of the $e\mu \to e\mu$ process as functions of the electron scattering angle $\cos\theta_{13}$ (left plot) and the muon scattering angle $\cos\theta_{24}$ (right plot). The ratio of the NLO and LO (left) and relative NLO QED corrections (right) are shown in the lower panels.

In Fig. 3.6, we show that the effect of NLO corrections to the differential cross-section (left plot) in the region of the $-1.0 \leq \cos\theta_{13} \leq 0.0$ is large. Especially, in the very small region (near -1.0) NLO result approximates ten times the LO one. In case $\cos\theta_{24}$ (right plot), the correction is much smaller than the $\cos\theta_{13}$ (lower than 20 [%]).

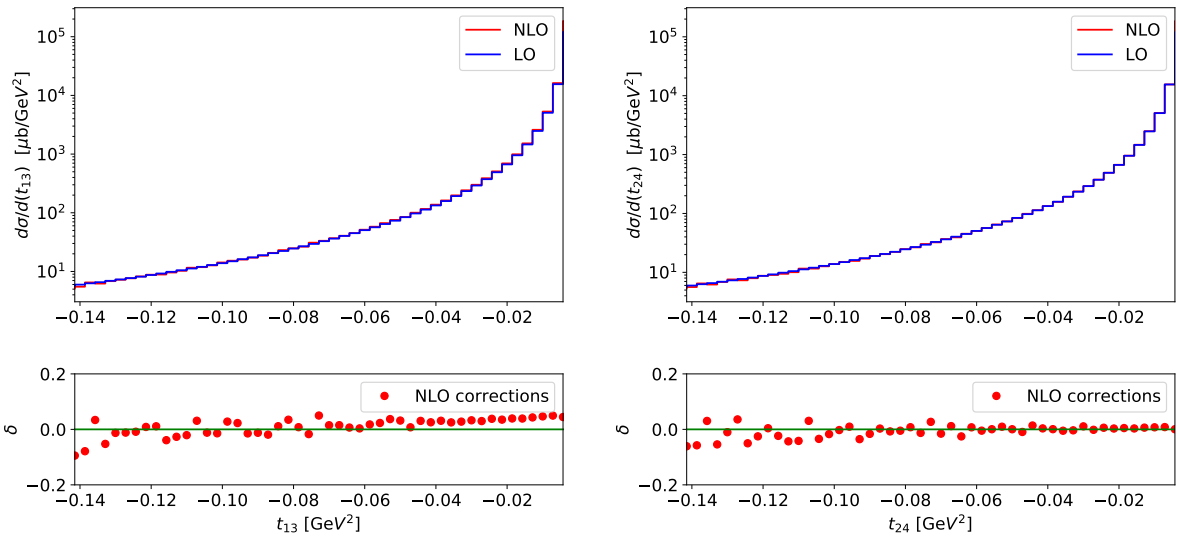

Figure 3.7: The LO and NLO QED differential cross-sections of the $e\mu \to e\mu$ process as functions of the squared momentum transfer $t_{13} = (p_1 - p_3)^2$ (left plot) and $t_{24} = (p_2 - p_4)^2$ (right plot). The relative NLO QED corrections are shown in the lower panels.

In Fig. 3.7, we see that the NLO corrections to the differential cross-section as a function of the squared momentum transfer t_{13} (left plot) and t_{24} (right plot) are small (less than 10 [%]).

CHAPTER

FOUR

CONCLUSION AND OUTLOOK

Conclusion

In this work, we have computed the cross-section of the bremsstrahlung process $e(p_1) + \mu(p_2) \to e(p_3) + \mu(p_4) + \gamma(k)$ in QED theory. This result together with the virtual + soft-photon corrections from Le Duc Truyen's thesis [6] gives the following NLO result:

$$\sigma_{\rm NLO}^{\rm QED} = 1335.2395 \pm 0.0061 \ [\mu{\rm b}],$$

with the cut on the energy of the final state electron $E_3 > 0.2$ [GeV] in the laboratory frame. The precision is 4.57 ppm obtained after 7 hours running the VEGAS+ code (using one core of the computer: Intel(R) Core(TM) i7-6700K CPU @ 4.00GHz).

To achieve this result, we use the newest version of VEGAS+ 4.0.3 and computed the cross-section without any approximations. Besides, we have constructed the three phase space mappings that are useful for cross checking numerical results. We have found that the mapping (34)5 gives the best precision.

We have also checked that the final NLO cross-section is independent of the soft-photon cut-off parameter ΔE.

Outlook

The next step is taking into account the pure weak contributions to obtain the full NLO results in the Standard Model.

APPENDIX

A

WICK THEOREM

A.0.1 Wick theorem

Considering S-matrix contain information about scattering transition probability [11] is:

$$S^{(n)} = \sum_{i=0}^{\infty} \frac{(-i)^n}{n!} \int_{-\infty}^{\infty} \dots \int_{-\infty}^{\infty} \mathcal{T}\{H_I(t_1)H_I(t_2)\dots H_I(t_n)\}\, \mathrm{d}^4x_1\, \mathrm{d}^4x_2 \dots \mathrm{d}^4x_n\,. \tag{A.1}$$

In QED, the interaction Hamiltonian $H_I(t) = e\bar{\psi}\gamma^\mu\psi A_\mu$. In the expansion of S-matrix contain the time ordered operator $\mathcal{T}$, in terms of which contain the normal ordered. The normal product operator is the procedure that putting all destruction operator in the right hand side of the creation operator. The time ordered operator is another differently which move all operator at the early time in right of operator in the later time, this cause the contrary between two operators. For this, we need the relation connection them which is **Wick's theorem** [16].

Consider the Wick's theorem in case two scalar fields. Based on the definition of time ordered operator:

$$\mathcal{T}[\phi(x)\phi(x')] \equiv \Theta(t-t')\phi(x)\phi(x') + \Theta(t'-t)\phi(x')\phi(x). \tag{A.2}$$

We have to write the right hand side (RHS) of Eq.(A.2) in term of normal product. It can be done by rewriting:

$$\phi(x) = \phi_+(x) + \phi_-(x). \tag{A.3}$$

where $\phi_+(x)$ contains the annihilation operator and $\phi_-(x)$ contains the creation operator in written explicitly.

$$\phi_+(x) = \int \frac{\mathrm{d}^3\mathbf{p}}{(2\pi)^3}\frac{1}{\sqrt{2E}} e^{-ipx} a_{\mathbf{p}}, \qquad \phi_-(x) = \int \frac{\mathrm{d}^3\mathbf{p}}{(2\pi)^3}\frac{1}{\sqrt{2E}} e^{ipx} a^+_{\mathbf{p}}. \tag{A.4}$$

Based on the properties of the quantum state, the annihilation operator acting on vacuum state and give the zero. We have:

$$\phi_+(x)\,|0\rangle = 0, \qquad \langle 0|\,\phi_-(x) = 0. \tag{A.5}$$

Then:

$$\phi(x)\phi(x') = \phi_+(x)\phi_+(x') + \phi_-(x)\phi_+(x') + \phi_+(x)\phi_-(x') + \phi_-(x)\phi_-(x'). \tag{A.6}$$

The normal ordered operator $:\phi(x)\phi(x'):$ is the same form of Eq.(A.6) except the third term:

$$\begin{aligned} :\phi(x)\phi(x'): &= \phi(x)\phi(x') - \phi_+(x)\phi_-(x') + \phi_-(x)\phi_+(x') && \text{(A.7)}\\ &= \phi(x)\phi(x') - [\phi_+(x), \phi_-(x)]_-. && \text{(A.8)} \end{aligned}$$

If we take both side of Eq. (A.6) inside the vacuum expectation. In other word:

$$\langle 0|\phi(x)\phi(x')|0\rangle = \langle 0|\phi_+(x)\phi_-(x')|0\rangle\,, \tag{A.9}$$

since the remaining term is vanish according to Eq. (A.5), we can rewrite the Eq. (A.9) by additional the extra term that annihilation the vacuum state:

$$\begin{aligned} \langle 0|\phi(x)\phi(x')|0\rangle &= \langle 0|\phi_+(x)\phi_-(x') - \phi_-(x')\phi_+(x)|0\rangle && \text{(A.10)}\\ \langle 0|\phi(x)\phi(x')|0\rangle &= \langle 0|[\phi_+(x), \phi_-(x')]_-|0\rangle\,. && \text{(A.11)} \end{aligned}$$

The vacuum expectation in Eq. (A.11) is a number because of the commutation relation in the RHS is also a number. It make sense when putting all together into Eq. (A.8):

$$\phi(x)\phi(x') =: \phi(x)\phi(x'): + \langle 0|[\phi_+(x), \phi_-(x')]_-|0\rangle\,. \tag{A.12}$$

Taking both side of Eq. (A.12) by time ordered operator we get:

$$\mathcal{T}[\phi(x)\phi(x')] =: \phi(x)\phi(x'): + \langle 0|\mathcal{T}[\phi_+(x), \phi_-(x')]_-|0\rangle\,. \tag{A.13}$$

The RHS of Eq. (A.13) contain the time ordering product of two field. It quantity can be rewritten simple by Wick contraction:

$$\langle 0|\mathcal{T}[\phi_+(x), \phi_-(x')]_-|0\rangle = \overbrace{\phi(x)\phi}(x'). \tag{A.14}$$

If they correspond to the same field. Get i times respect to the Feynman propagator [16]:

$$\begin{aligned} \overbrace{\phi(x_1)\phi}(x_2) &= i\Delta^F(x_1 - x_2), && \text{(A.15)}\\ \overbrace{\phi(x_1)\phi^\dagger}(x_2) &= \overbrace{\phi^\dagger(x_2)\phi}(x_1) = i\Delta^F(x_1 - x_2), && \text{(A.16)}\\ \overbrace{\psi_\alpha(x_1)\overline{\psi}_\beta}(x_2) &= -\overbrace{\psi_\beta(x_2)\psi_\alpha}(x_1) = iS^F_{\alpha\beta}(x_1 - x_2), && \text{(A.17)}\\ \overbrace{A_\mu(x_1)A_\nu}(x_2) &= iD^F_{\mu\nu}(x_1 - x_2). && \text{(A.18)} \end{aligned}$$

A.0.2 Third-order of S-matrix

The Bremsstrahlung scattering:

$$e(p_1) + \mu(p_2) \to e(p_3) + \mu(p_4) + \gamma(k) \tag{A.19}$$

where the initial and final state is defined as:

$$\begin{aligned} |p_1p_2\rangle &= \sqrt{2E_1}\sqrt{2E_2}a^{\dagger s_1}_{\mathbf{p}_1}a^{\dagger s_2}_{\mathbf{p}_2}\,|0\rangle\,, && \text{(A.20)}\\ \langle p_3p_4k| &= \langle 0|\,\sqrt{2E_3}\sqrt{2E_4}\sqrt{2k_0}a^{s_3}_{\mathbf{p}_3}a^{s_4}_{\mathbf{p}_4}a^{\lambda}_{\mathbf{k}}. && \text{(A.21)} \end{aligned}$$

From the interaction term in Eq. (1.2):

$$\mathcal{L}_{int} = -e\bar{\psi}(x)\gamma^{\mu}\psi(x)A_{\mu}(x), \tag{A.22}$$

The first non-trivial contribute to amplitude obtained with the $S^{(3)}$. We have the formula of amplitude scattering is:

$$\langle p_3 p_4 k|S^{(3)} - 1|p_1 p_2\rangle = lim_{T\to\infty}\,\langle p_3 p_4 k|\mathcal{T}\left[exp\left(-i\int_{-T}^{T} dt\mathcal{H}_i\right)\right]|p_1 p_2\rangle\,. \tag{A.23}$$

where $\mathcal{H}_i = e\int \mathrm{d}^3x\left(\bar{\psi}_e^x\gamma^{\alpha}\psi_e^x A_{\alpha}^x + \bar{\psi}_{\mu}^x\gamma^{\alpha}\psi_{\mu}^x A_{\alpha}^x\right)$. We have:

$$\begin{aligned}
&\langle p_3 p_4 k|S^{(3)} - 1|p_1 p_2\rangle = \\
&\langle p_3 p_4 k|\,\frac{1}{3!}(-ie)^3\int \mathrm{d}^4x\,\mathrm{d}^4y\,\mathrm{d}^4z\,\mathcal{T}\{[\left(\bar{\psi}_e^x\gamma^{\alpha}\psi_e^x A_{\alpha}^x + \bar{\psi}_{\mu}^x\gamma^{\alpha}\psi_{\mu}^x A_{\alpha}^x\right)\\
&\times\left(\bar{\psi}_e^y\gamma^{\beta}\psi_e^y A_{\beta}^y + \bar{\psi}_{\mu}^y\gamma^{\beta}\psi_{\mu}^y A_{\beta}^y\right)\left(\bar{\psi}_e^z\gamma^{\nu}\psi_e^z A_{\nu}^z + \bar{\psi}_{\mu}^z\gamma^{\nu}\psi_{\nu}^z A_{\nu}^z\right)]\}\,|p_1 p_2\rangle\\
&= i\mathcal{M}(2\pi)^4\delta^4(p_i - p_f).
\end{aligned} \tag{A.24}$$

Among the eight terms occurring in Eq. (A.24) and considering the symmetry of x,y,z. So, we reduce the factor 1/3 and get two terms contribution to the scattering A.19:

$$\bar{\psi}_e^x\gamma^{\alpha}\psi_e^x A_{\alpha}^x\bar{\psi}_e^y\gamma^{\beta}\psi_e^y A_{\beta}^y\bar{\psi}_{\mu}^z\gamma^{\nu}\psi_{\mu}^z A_{\nu}^z, \tag{A.25}$$

$$\bar{\psi}_{\mu}^x\gamma^{\alpha}\psi_{\mu}^x A_{\alpha}^x\bar{\psi}_{\mu}^y\gamma^{\beta}\psi_{\mu}^y A_{\beta}^y\bar{\psi}_e^z\gamma^{\nu}\psi_e^z A_{\nu}^z. \tag{A.26}$$

Then third-order S-matrix expand:

$$\begin{aligned}
&\langle p_3 p_4 k|S^{(3)} - 1|p_1 p_2\rangle = \\
&(-ie)^3\frac{1}{2}\int \mathrm{d}^4x\,\mathrm{d}^4y\,\mathrm{d}^4z\,\langle p_3 p_4 k|\,\mathcal{T}\{[\bar{\psi}_e^x\gamma^{\alpha}\psi_e^x A_{\alpha}^x\bar{\psi}_e^y\gamma^{\beta}\psi_e^y A_{\beta}^y\bar{\psi}_{\mu}^z\gamma^{\nu}\psi_{\mu}^z A_{\nu}^z\\
&+ \bar{\psi}_{\mu}^x\gamma^{\alpha}\psi_{\mu}^x A_{\alpha}^x\bar{\psi}_{\mu}^y\gamma^{\beta}\psi_{\mu}^y A_{\beta}^y\bar{\psi}_e^z\gamma^{\nu}\psi_e^z A_{\nu}^z]\}\,|p_1 p_2\rangle\,.
\end{aligned} \tag{A.27}$$

where the field operator of the fermion field and the photon field [11]:

$$\psi(x) = \int\frac{\mathrm{d}^3\mathbf{p}}{(2\pi)^3\sqrt{2E}}\sum_s\left(a_{\mathbf{p}}^s u^s(p)e^{-ipx} + b_{\mathbf{p}}^{\dagger s}v^s(p)e^{ipx}\right), \tag{A.28}$$

$$\bar{\psi}(x) = \int\frac{\mathrm{d}^3\mathbf{p}}{(2\pi)^3\sqrt{2E}}\sum_s\left(a_{\mathbf{p}}^{\dagger s}\bar{u}^s(p)e^{ipx} + b_{\mathbf{p}}^s\bar{v}^s(p)e^{ipx}\right), \tag{A.29}$$

$$A(x) = \int\frac{\mathrm{d}^3\mathbf{x}}{(2\pi)^3\sqrt{2k_0}}\sum_{\lambda}\left(a_{\mathbf{k}}^{\lambda}\epsilon^{\lambda}(k)e^{-ikx} + a_{\mathbf{k}}^{\dagger\lambda}\epsilon^{*\lambda}(k)e^{ikx}\right). \tag{A.30}$$

We now analyze separately time ordering operator in Eq. (A.25):

$$\begin{aligned}
\mathcal{T}[\bar{\psi}_e^x\gamma^{\alpha}\psi_e^x A_{\alpha}^x\bar{\psi}_e^y\gamma^{\beta}\psi_e^y A_{\beta}^y\bar{\psi}_{\mu}^z\gamma^{\nu}\psi_{\mu}^z A_{\nu}^z] &= 2\overbrace{\psi_e^x\bar{\psi}_e^y}A_{\alpha}^x\overbrace{A_{\nu}^z}\times:\bar{\psi}_e^x\gamma^{\alpha}\gamma^{\beta}\psi_e^y A_{\beta}^y\bar{\psi}_{\mu}^z\gamma^{\nu}\psi_{\mu}^z:\\
&+ 2\overbrace{\psi_e^x\bar{\psi}_e^y}A_{\beta}^y\overbrace{A_{\nu}^z}\times:\bar{\psi}_e^x\gamma^{\alpha}A_{\alpha}^x\gamma^{\beta}\psi_e^y\bar{\psi}_{\mu}^z\gamma^{\nu}\psi_{\mu}^z:,
\end{aligned} \tag{A.31}$$

And similarly in Eq. (A.26)

$$\begin{aligned}\mathcal{T}[\bar{\psi}^x_\mu\gamma^\alpha\psi^x_\mu A^x_\alpha\bar{\psi}^y_\mu\gamma^\beta\psi^y_\mu A^y_\beta\bar{\psi}^z_e\gamma^\nu\psi^z_e A^z_\nu] = 2\overbrace{\psi^x_\mu\bar{\psi}^y_\mu}A^x_\alpha A^z_\nu\times:\bar{\psi}^x_\mu\gamma^\alpha\gamma^\beta\psi^y_\mu A^y_\beta\bar{\psi}^z_e\gamma^\nu\psi^z_e: \\ + 2\overbrace{\psi^x_\mu\bar{\psi}^y_\mu}A^y_\beta A^z_\nu\times:\bar{\psi}^x_\mu\gamma^\alpha A^x_\alpha\gamma^\beta\psi^y_\mu\bar{\psi}^z_e\gamma^\nu\psi^z_e:.\end{aligned} \tag{A.32}$$

The factor 2 derive from the analogous perturbation of the fermion operator. Then we take out the factor 1/2 in Eq. (A.32) Taking the first term in the right hand side (RHS) of Eq. (A.31) into the initial and final states of the scattering (A.19), we obtain:

$$\begin{aligned}I =\ & \langle p_3p_4k|\overbrace{\psi^x_e\bar{\psi}^y_e}A^x_\alpha A^z_\nu\times:\bar{\psi}^x_e\gamma^\alpha\gamma^\beta\psi^y_e A^y_\beta\bar{\psi}^z_\mu\gamma^\nu\psi^z_\mu:|p_1p_2\rangle = \\ & (-ie)^3\int\frac{\mathrm{d}^3\mathbf{q}_1}{\sqrt{2E_{q_1}}}\frac{\mathrm{d}^3\mathbf{q}_2}{\sqrt{2E_{q_2}}}\frac{\mathrm{d}^3\mathbf{q}_3}{\sqrt{2E_{q_3}}}\frac{\mathrm{d}^3\mathbf{q}_4}{\sqrt{2E_{q_4}}}\frac{\mathrm{d}^3\mathbf{k}'}{\sqrt{2k'_0}}\int\mathrm{d}^4x\,\mathrm{d}^4y\,\mathrm{d}^4z \\ & \times\sqrt{2E_{\mathbf{p}_1}}\sqrt{2E_{\mathbf{p}_2}}\sqrt{2E_{\mathbf{p}_3}}\sqrt{2E_{\mathbf{p}_4}}\sqrt{2E_{\mathbf{k}'}} \\ & \times\langle 0|a^\lambda_{\mathbf{k}}a^{s_4}_{\mathbf{p}_4}a^{s_3}_{\mathbf{p}_3}a^{r_3}_{\mathbf{q}_3}a^{r_1}_{\mathbf{q}_1}a^{\lambda'}_{\mathbf{k}'}a^{r_4}_{\mathbf{q}_4}a^{r_2}_{\mathbf{q}_2}a^{s_1}_{\mathbf{p}_1}a^{s_2}_{\mathbf{p}_2}|0\rangle \\ & \times(\bar{u}^{r_3}(q_3)\gamma^\alpha\epsilon^{*\lambda}_\alpha\int\frac{\mathrm{d}^4q_3}{(2\pi)^4}\frac{i}{\not{q}_2-m_e}\gamma^\beta u^{r_1}(q_1)\int\frac{\mathrm{d}^4q'}{(2\pi)^4}\frac{-ig_{\beta\nu}}{q'^2_1}\bar{u}^{r_4}(q_4)\gamma^\nu u^{r_2}(q_2)) \\ & \times e^{ix(q_3+k-q)}e^{iy(q-q_1-q')}e^{iz(q'+q_4-q_2)}.\end{aligned} \tag{A.33}$$

Using the anticommutation relation of annihilation and creation operator of fermion field and commutation relation of creation and destruction operator of photon field:

$$\left\{a^r_{\mathbf{p}},a^{\dagger s}_{\mathbf{q}}\right\} = (2\pi)^3\delta^3(\mathbf{p}-\mathbf{q})\delta^{rs}, \tag{A.34}$$

$$\left[a^\lambda_{\mathbf{p}},a^{\lambda'}_{\mathbf{q}}\right] = (2\pi)^3\delta^3(\mathbf{p}-\mathbf{q})\delta^{\lambda\lambda'}. \tag{A.35}$$

We have:

$$\begin{aligned}I =\ & (-ie)^3\int\frac{\mathrm{d}^3\mathbf{q}_1}{\sqrt{2E_{q_1}}}\frac{\mathrm{d}^3\mathbf{q}_2}{\sqrt{2E_{q_2}}}\frac{\mathrm{d}^3\mathbf{q}_3}{\sqrt{2E_{q_3}}}\frac{\mathrm{d}^3\mathbf{q}_4}{\sqrt{2E_{q_4}}}\frac{\mathrm{d}^3\mathbf{k}'}{\sqrt{2k'_0}}\times\int\mathrm{d}^4x\,\mathrm{d}^4y\,\mathrm{d}^4z \\ & \times\sqrt{2E_{\mathbf{p}_1}}\sqrt{2E_{\mathbf{p}_2}}\sqrt{2E_{\mathbf{p}_3}}\sqrt{2E_{\mathbf{p}_4}}\sqrt{2E_{\mathbf{k}'}} \\ & \times(2\pi)^3(p_3-q_3)\delta^{s_3r_3}(2\pi)^3(p_1-q_1)\delta^{s_1r_1}(2\pi)^3(p_4-q_4)\delta^{s_4r_4}(2\pi)^3(p_2-q_2)\delta^{s_2r_2} \\ & \times(2\pi)^3(k-k')\delta^{\lambda\lambda'} \\ =\ & [\frac{\mathrm{d}^4q_3}{(2\pi)^4}\int\frac{\mathrm{d}^4q'}{(2\pi)^4}(\bar{u}^{r_3}(q_3)\gamma^\alpha\epsilon^{*\lambda}_\alpha\frac{1}{\not{q}_2-m_e}\gamma^\beta u^{r_1}(q_1)\frac{g_{\beta\nu}}{q'^2_1}\bar{u}^{r_4}(q_4)e^{iq_4z}\gamma^\nu u^{r_2}(q_2))] \\ & \times\delta^4(p_3+k'-q)\delta^4(q-p_1-q')\delta^4(q'+p_4-p_2).\end{aligned} \tag{A.36}$$

we get:

$$
\begin{aligned}
I &= (-ie)^3 \int \frac{\mathrm{d}^3\mathbf{q}_1}{\sqrt{2E_{q_1}}} \frac{\mathrm{d}^3\mathbf{q}_2}{\sqrt{2E_{q_2}}} \frac{\mathrm{d}^3\mathbf{q}_3}{\sqrt{2E_{q_3}}} \frac{\mathrm{d}^3\mathbf{q}_4}{\sqrt{2E_{q_4}}} \frac{\mathrm{d}^3\mathbf{k}'}{\sqrt{2k'_0}} \times \int \mathrm{d}^4x\, \mathrm{d}^4y\, \mathrm{d}^4z \\
&\times \sqrt{2E_{\mathbf{p}_1}}\sqrt{2E_{\mathbf{p}_2}}\sqrt{2E_{\mathbf{p}_3}}\sqrt{2E_{\mathbf{p}_4}}\sqrt{2E_{\mathbf{k}'}} \\
&\times (2\pi)^3(p_3-q_3)\delta^{s_3r_3}(2\pi)^3(p_1-q_1)\delta^{s_1r_1}(2\pi)^3(p_4-q_4)\delta^{s_4r_4}(2\pi)^3(p_2-q_2)\delta^{s_2r_2} \\
&\times (2\pi)^3(k-k')\delta^{\lambda\lambda'} \\
&= [\frac{\mathrm{d}^4q_3}{(2\pi)^4}\int \frac{\mathrm{d}^4q'}{(2\pi)^4}(\bar{u}^{r_3}(q_3)\gamma^\alpha\epsilon^{*\lambda}_\alpha \frac{1}{\not{q}_2 - m_e}\gamma^\beta u^{r_1}(q_1)\frac{-g_{\beta\nu}}{q_1'^2}\bar{u}^{r_4}(q_4)e^{iq_4z}\gamma^\nu u^{r_2}(q_2))] \\
&\times \delta^4(p_3+k'-q)\delta^4(q-p_1-q')\delta^4(q'+p_4-p_2) \\
&= (-ie)^3(2\pi)^4[\bar{u}^{r_3}(q_3)\gamma^\alpha\epsilon^{*\lambda}_\alpha \frac{1}{\not{q}_2 - m_e}\gamma^\beta u^{r_1}(q_1)\frac{g_{\beta\nu}}{q_1'^2}\bar{u}^{r_4}(q_4)\gamma^\nu u^{r_2}(q_2)] \\
&\times \delta^4(p_3-p_1+k+p_4-p_2).
\end{aligned}
\tag{A.37}
$$

where:

$$
\begin{cases}
\mathbf{q_2} = \mathbf{p_3} + \mathbf{k}, \\
\mathbf{q'}_1 = \mathbf{p_2} - \mathbf{p_4}.
\end{cases}
$$

Then, one of the Feynman amplitude of $e\mu \to e\mu\gamma$ process is obtained from Eq. (A.24):

$$
\mathcal{M}_2 = -ie^3[\bar{u}^{r_3}(q_3)\gamma^\alpha\epsilon^{*\lambda}_\alpha \frac{1}{\not{q}_2 - m_e}\gamma^\beta u^{r_1}(q_1)\frac{g_{\beta\nu}}{q_1'^2}\bar{u}^{r_4}(q_4)\gamma^\nu u^{r_2}(q_2)]. \tag{A.38}
$$

Doing the flowing procedure above to obtain the remaining results. The second term of Eq. (A.31) is:

$$
\mathcal{M}_1 = ie^3[\bar{u}^{r_3}(q_3)\gamma^\beta \frac{1}{\not{q}_1 - m_e}\gamma^\alpha\epsilon^{*\lambda}_\alpha u^{r_1}(q_1)\frac{g_{\beta\nu}}{q_1'^2}\bar{u}^{r_4}(q_4)\gamma^\nu u^{r_2}(q_2)], \tag{A.39}
$$

where:

$$
\mathbf{q_1} = \mathbf{p_1} + \mathbf{k}. \tag{A.40}
$$

The first term of Eq. (A.32):

$$
\mathcal{M}_3 = ie^3[\bar{u}^{r_4}(q_4)\gamma^\beta \frac{1}{\not{q}_3 - m_e}\gamma^\alpha\epsilon^{*\lambda}_\alpha u^{r_2}(q_2)\frac{g_{\beta\nu}}{q_2'^2}\bar{u}^{r_3}(q_3)\gamma^\nu u^{r_1}(q_1)], \tag{A.41}
$$

where:

$$
\begin{cases}
\mathbf{q_3} = \mathbf{p_2} + \mathbf{k}, \\
\mathbf{q'}_2 = \mathbf{p_1} - \mathbf{p_3}.
\end{cases}
$$

And the last term of Eq. (A.32):

$$
\mathcal{M}_4 = ie^3[\bar{u}^{r_4}(q_4)\gamma^\alpha\epsilon^{*\lambda}_\alpha \frac{1}{\not{q}_4 - m_\mu}\gamma^\beta u^{r_2}(q_2)\frac{g_{\beta\nu}}{q_2'^2}\bar{u}^{r_3}(q_3)\gamma^\nu u^{r_1}(q_1)], \tag{A.42}
$$

where

$$
\mathbf{q_4} = \mathbf{p_4} + \mathbf{k}. \tag{A.43}
$$

APPENDIX

B

LORENTZ TRANSFORMATION

Consider two reference frames S defined by coordinates t, x, y, z; S' and its coordinates t', x', y', z' move relative to S with constant velocity $\mathbf{v}$ along side the z axis. The relationship between two system of references is Lorentz transformation [12]. For simplicity, x, x' and y, y' axis still parallel to each other, the time is synchronize at origin $t' = t = 0$ and use the natural unit $\hbar = c = 1$ for all.

$$x' = x, \tag{B.1}$$
$$y' = y, \tag{B.2}$$
$$z' = \gamma(z - vt), \tag{B.3}$$
$$t = \gamma(t - vz), \tag{B.4}$$

where γ is Lorentz factor.

$$\gamma = (1 - v^2)^{-1/2}. \tag{B.5}$$

If the relative velocity between two frames in arbitrary direction, generally form of Lorentz transformation according to Ref. [12]:

$$\mathbf{w}' = \mathbf{w} + \gamma\mathbf{x}\left(\frac{\gamma\mathbf{v}.\mathbf{w}}{\gamma + 1} - t\right), \tag{B.6}$$
$$t = \gamma(t - \mathbf{v}.\mathbf{w}). \tag{B.7}$$

where $\mathbf{w} = (x, y, z)$.
Based on the theory of special relativity the three components of space x, y, z and time t construct the four-vector $x^\mu = (x^0, x^1, x^2, x^3) = (t, x, y, z)$. Under Lorentz transformation any four-vector $a^\nu = (a^0, a^1, a^2, a^3)$ transform like x Ref. [12]. Therefore, the Eq. (B.6) and Eq. (B.7) is rewritten in terms of the four-momentum $p^\mu = (E, \mathbf{p})$ is:

$$\mathbf{p}' = \mathbf{p} + \gamma\mathbf{x}\left(\frac{\gamma\mathbf{v}.\mathbf{p}}{\gamma + 1} - E\right), \tag{B.8}$$
$$E' = \gamma(E - \mathbf{v}.\mathbf{p}). \tag{B.9}$$

According to Ref. [12], the momentum and energy are related to the velocity and Lorentz factor is:

$$\mathbf{v} = \frac{\mathbf{p}}{E}, \tag{B.10}$$

$$\gamma = \frac{E}{m}, \tag{B.11}$$

$$v\gamma = \frac{\mathbf{p}}{m}. \tag{B.12}$$

Numerical simplification require change Eq. (B.8) and Eq. (B.9) into the matrix form $p' = Lp$, which L stand for Lorentz transformation matrix:

$$\mathbf{v} = (v_x, v_y, v_z) \tag{B.13}$$

$$v^2 = v_x^2 + v_y^2 + v_z^2 \tag{B.14}$$

$$p = (E, p_x, p_y, p_z) \tag{B.15}$$

$$p' = (E', p'_x, p'_y, p'_z) \tag{B.16}$$

According to Ref. [17]:

$$\begin{pmatrix} E' \\ p'_x \\ p'_y \\ p'_z \end{pmatrix} = \begin{pmatrix} \gamma & -\gamma v_x & -\gamma v_y & -\gamma v_z \\ -\gamma v_x & 1+(\gamma+1)\frac{v_x^2}{v^2} & (\gamma+1)\frac{v_x v_y}{v^2} & (\gamma+1)\frac{v_x v_z}{v^2} \\ -\gamma v_y & (\gamma+1)\frac{v_x v_y}{v^2} & 1+(\gamma+1)\frac{v_y^2}{v^2} & (\gamma+1)\frac{v_y v_z}{v^2} \\ -\gamma v_z & (\gamma+1)\frac{v_x v_z}{v^2} & (\gamma+1)\frac{v_y v_z}{v^2} & 1+(\gamma+1)\frac{v_z^2}{v^2} \end{pmatrix} \begin{pmatrix} E \\ p_x \\ p_y \\ p_z \end{pmatrix} \tag{B.17}$$

APPENDIX

C

VEGAS+, BASES AND FORM

C.0.1 VEGAS+

VEGAS+ is the computing multidimensional integral using the VEGAS+'s algorithm Ref. [9]. The advantage of VEGAS+ is the function below the integration need not be analytic or even continue.

From the technical point of view, we first analyze the important parameters when working on VEGAS+ and how to improve the efficiency of convergence behavior by controlling them.

For instance, the Python program compute the two-dimensional $f(x, y) = xy$, with $x = [0, 2]$, $y = [0, 3]$ with VEGAS+.

Listing C.1: Python program define f(x)

```
import numpy as np
import vegas

#Define f(x) = xy with x[0] stand for x
#and x[1] stand for y
def f(x):
para_1 = x[0]
para_2 = x[1]
result  = para_1*para_2
```

Listing C.2: Main integration computing f(x)

```
return result
#Main program of estimating integral
#call vegas and region of the integral. First braket is
#the range of x and second is the range of y
np.random.seed([1,2])
iteg = vegas.Integrator([[0.,2.],[0.,3.]])

#Training
#Step_1 -- adapt to f, discard the result
iteg(f,nitn = 5, neval = 1000,alpha = 0.6)

#Calculating
#Step_2 -- iteg has adapt to f , keep result
result = iteg(f,nitn = 5, neval = 1000,alpha = 0.4)
print('Calculating!!!')
print(result.summary())

print('result=%s ;Q=%.2f ' % (result, result.Q))
```

First we defined the integrand $f(x, y) = xy$ in Listing (C.1) and then create the integrator in Listing (C.2) , *iteg*, which is the integration operator that apply to the two-dimensional function $f(x, y)$. Finally, we apply to our integrated $f(x)$, calling the VEGAS+ to estimate the integral using nint = 10 iterations, each of which uses neval = 1000 evaluations of the integrand. The line np.random.seed([1,2]) is fixed the random number generate by VEGAS+ algorithm the value [1,2] is convenient choose for modifying code or calculating the convergence rate of the phase space mappings not only different points but also different nitn. The damping parameter alpha = 0.6 in training step and alpha = 0.4 in integration step (the default value of alpha = 0.5) control the speed with VEGAS+ adapts. We do the following steps for improving the results of VEGAS+:

1. Setting training integrator and discarding the result from the first run time is a better efficient way because VEGAS+ can find the early peak and improve the convergence adaption in the second time.

2. Setting the value of alpha is large (0.5 < alpha < 1.0) in the training step and the slower alpha's value (0 < alpha < 0.3) in the integration step, which makes calculating integral is more efficient.

The result format by follow:

1. The call result.summary() returns a summary of results from each iteration.

2. The result.Q is p-value of the weighted average's $\chi 2$,which is the probability that a larger χ^2 could result from random (Gaussian) fluctuations

Listing C.3: VEGAS+ result

```
Calculating!!!
itn   integral        wgt average     chi2/dof        Q
-------------------------------------------------------
1   8.982(18)       8.982(18)           0.00      1.00
2   8.994(18)       8.988(12)           0.22      0.64
3   8.971(18)       8.982(10)           0.43      0.65
4   9.018(14)       8.9947(82)          1.76      0.15
5   9.006(13)       8.9978(70)          1.45      0.21

result=8.9978(70)  ; Q=0.21
```

The first column represent the number of iterations, the next is the value of integrad obtained by VEGAS+. The weight average (wgt average) $\bar{K}$ minimizes:

$$\chi^2 = chi2 = \sum_i \frac{(K_i - \bar{K})}{\epsilon_i^2} \tag{C.1}$$

Where $K_i + \epsilon_i$ are the result from individual iterations. If the K_i is Gaussian, $\chi 2$ should be of the order of degree of freedom (The common choice is chi2/dof < 1.0). and Q choose in the range $[0.2, 0.9]$ (when any iteration has $0.0 \leq Q \leq 0.1$ we have to discard the result and reduce the value of alpha).

C.0.2 BASES

Similar to VEGAS+, BASES is also the multidimensional integral [8] but it is written in FORTRAN language (VEGAS+ is in Python). In the early procedure, BASES do the step "Gird Optimize" that find the high probability distribution of the integration function $f(x)$, then adapt the grid to estimate integration.

Listing C.4: Fortran code in 2-dimensional integration

```
!Define the function f(x,y) = x*y

real*8 Function f(x)
Implicit none
Integer, PARAMETER:: dim = 50 ! Maximum variables using in BASES
real*8 x(dim)
real*8 xmax, xmin, ymax, ymin, jaco, x1, x2
!x1 stand for x, x2 stand for y
xmax = 2d0
xmin = 0d0
ymax = 3d0
ymin = 0d0
! Change x integral in range [0,2] to [0,1]
!and y in range [0,3] to [0,1]
x1 = xmin  + (xmax - xmin)*x(1)
x2 = ymin  + (ymax - ymin)*x(2)

!Jacobian
```

```
jaco = (xmax - xmin)*(ymax - ymin)
f = jaco*x1*x2

End Function f
! Main program calculating integral

Program main
Implicit none
! Block subroutine and parameters using in BASES
Integer NDIMEN,NWILD
Integer*8 NCALL
Integer ,PARAMETER:: MXDIM = 50
Integer IG(MXDIM),ITMX1,ITMX2

real*8 XL(MXDIM),XU(MXDIM)
real*8 ACC1,ACC2,CTIME
Integer IT1, IT2
Integer ISEED_FLAG, ISEED_IN
Integer i

! common blocks are used to pass information to BASES
COMMON /BPARM0/ ISEED_FLAG, ISEED_IN
COMMON /BPARM1/ XL,XU,NDIMEN,NWILD,IG,NCALL
COMMON /BPARM2/ ACC1,ACC2,ITMX1,ITMX2

real*8 f
external f

real*8 result,error
Print*, "Hello World !!!"

! pass random-number seed to BASES
ISEED_FLAG = 1   ! choose 1 to change the default
! Seed value, else otherwise
ISEED_IN   = 1   ! choose an integral number for seed
Print*,"ISEED_IN =", ISEED_IN

!===> Initialization of BASES by calling BSINIT
CALL BSINIT

NDIMEN= 2      ! Numer of variables
NWILD = 2      ! Numer of variables are hard to integrate
NCALL = 1000   ! Number of evaluation points
ITMX1 = 10     ! number of iterations for finding the grid
ACC1  = 2D-3   ! Expectation relative error in "Grid Optimization"
ITMX2 = 10     ! number of iterations for "Final Integration step"
ACC2  = 1D-4   ! Expectation relative error in the Integration step
```

```
! Ranges for generating random numbers:
do i = 1, NDIMEN
XL(i)= 0D0
XU(i)= 1D0
end do

!![Initialization of Histograms
! Nbin = 50 ! maximally 50 bins

! Call bases and calculating integral
call BASES(f, result, error, CTIME, IT1, IT2)

Print*,"result =", result
Print*,"error  =", error

End Program main
```

The final result by BASES is:

Listing C.5: BASES result

```
Convergency Behavior for the Integration Step
IT  Eff  R_Neg    Estimate   Acc %  Estimate(+- Error )order   Acc %
-------------------------------------------------------------------
1  100   0.00   9.006E+00   0.378   9.005559(+-0.034033)E 00   0.378
2  100   0.00   9.023E+00   0.394   9.013977(+-0.024581)E 00   0.273
3  100   0.00   8.992E+00   0.347   9.005599(+-0.019313)E 00   0.214
4  100   0.00   9.037E+00   0.421   9.012053(+-0.017221)E 00   0.191
5  100   0.00   8.989E+00   0.327   9.006052(+-0.014857)E 00   0.165
-------------------------------------------------------------------
result =    9.0060516298778683
error  =    1.4856700592820505E-002
```

The first column is the number of iteration. The Efficient (Eff) of an algorithm is the percent of the certain points in the evaluation points for each iterations. The integral result in a specific step in Estimate. The first Acc % represents the absolute error from iteration to iteration or the variation of the present iteration to the next iteration. The last Acc % is the relative error of individual steps of integrated computing.
The last Appendix C.0.3 is the Form code to calculate the amplitude squared of the bremsstrahlung scattering.

C.0.3 FORM

```
*************************************
*Variables use in program          ***
*************************************
cfunction Ub,Vb,m,eps,dotp;
function U,V;
funpowers allfunpowers;
autodeclare vector p,h,k,q;
autodeclare symbol d;
index i,j,al,be,ga,mu,nu,rho,sig;
symbol mm, me, mm2, mm4, me2, me4;
symbol Fac1,Fac2, Fac3 , Fac4 ;

*************************************************************
*                                                           *
*process e (p1) + muon (p2) > e (p3) + muon (p4) + gamma (k) *
*                                                           *
*************************************************************
*Fac1 = e^3/((p3 + k)^2 - me^2)*(p2 - p4)^2)
*Fac2 = e^3/((p1 - k)^2 - me^2)*(p2 - p4)^2)
*Fac3 = e^3/((p4 + k)^2 - mm^2)*(p1 - p3)^2)
*Fac4 = e^3/((p2 - k)^2 - mm^2)*(p1 - p3)^2)

*********************************************************
*                              gamma(k)                 *
*                            *                          *
*                           *                           *
*                          *                            *
*     e(p1) *******>****>**********>******** e(p3)      *
*                              *                        *
*                              *                        *
*                              *                        *
* muon(p2) *******>**************>******** muon(p4)    *
*                                                       *
*********************************************************
local [M1] = Fac2*Ub(1,p3)*g_(1,be)*(g_(1,p1) - g_(1,k) + me)*
g_(1,al)*U(1,p1)*Ub(2,p4)*g_(2,be)*U(2,p2);
```

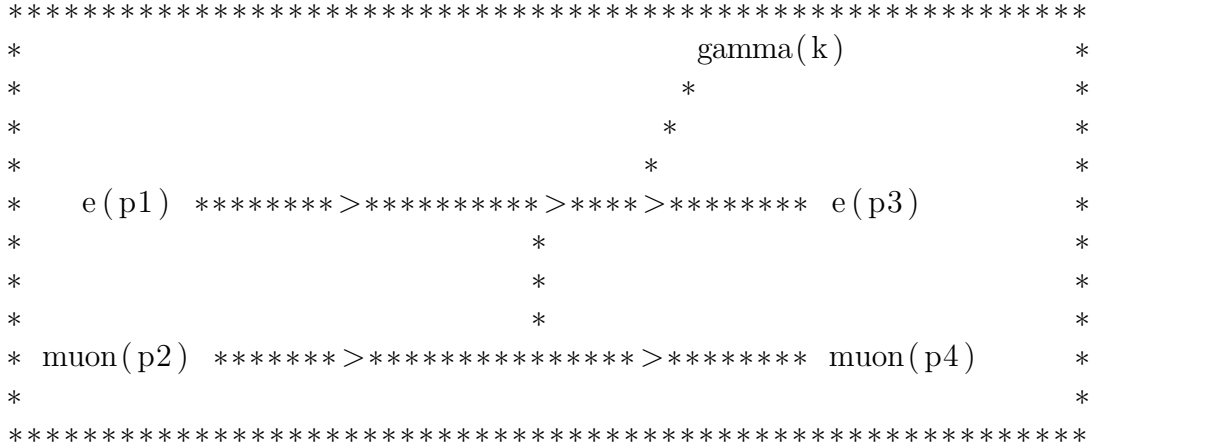


```
local [M2] = Fac1*Ub(1,p3)*g_(1,al)*(g_(1,p3) + g_(1,k) + me)*
g_(1,be)*U(1,p1)*Ub(2,p4)*g_(2,be)*U(2,p2);
```

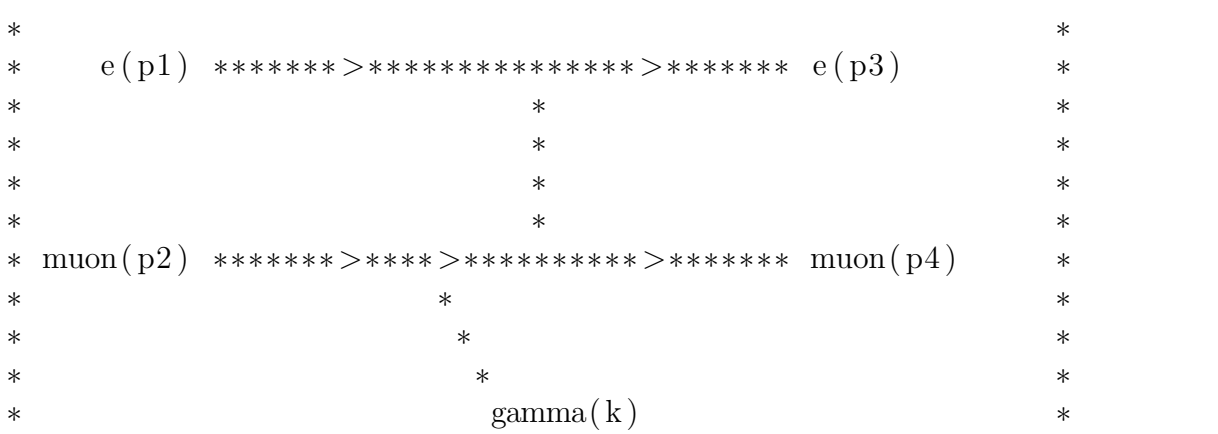


```
local [M3]= Fac4*Ub(2,p4)*g_(2,be)*(g_(2,p2) - g_(2,k) + mm)*
g_(2,al)*U(2,p2)*Ub(1,p3)*g_(1,be)*U(1,p1);
```

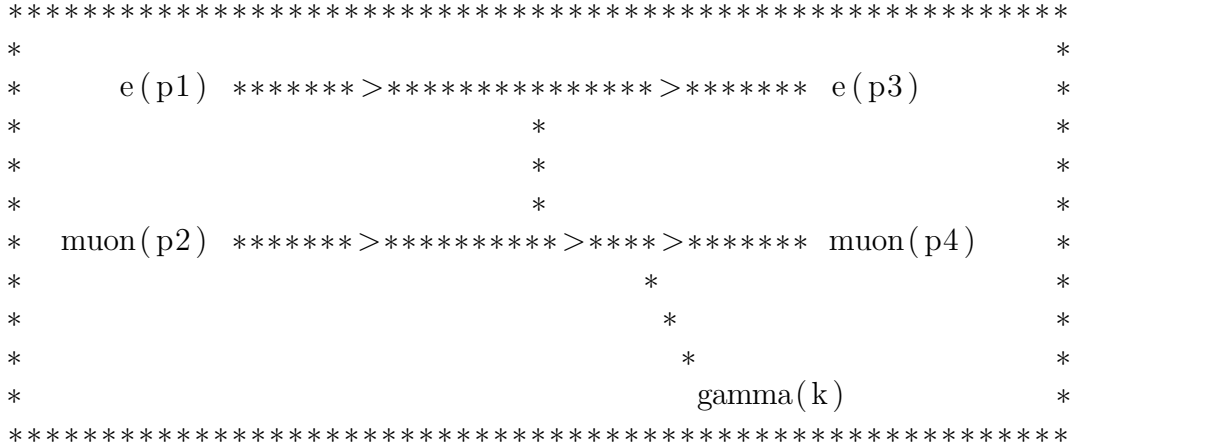


```
local [M4] = Fac3*Ub(2,p4)*g_(2,al)*(g_(2,p4) + g_(2,k) + mm)*
g_(2,be)*U(2,p2)*Ub(1,p3)*g_(1,be)*U(1,p1);

local [M1*]= Fac2*Ub(1,p1)*g_(1,mu)*(g_(1,p1) - g_(1,k) + me)*
g_(1,nu)*U(1,p3)*Ub(2,p2)*g_(2,nu)*U(2,p4);
```

```
local [M2*] = Fac1*Ub(1,p1)*g_(1,nu)*(g_(1,p3) + g_(1,k) + me)*
g_(1,mu)*U(1,p3)*Ub(2,p2)*g_(2,nu)*U(2,p4);

local [M3*] = Fac4*Ub(2,p2)*g_(2,mu)*(g_(2,p2) - g_(2,k) + mm)*
g_(2,nu)*U(2,p4)*Ub(1,p1)*g_(1,nu)*U(1,p3);

local [M4*] = Fac3*Ub(2,p2)*g_(2,nu)*(g_(2,p4) + g_(2,k) + mm)*
g_(2,mu)*U(2,p4)*Ub(1,p1)*g_(1,nu)*U(1,p3);


*print;
.sort

*************************************************
*Sum over polarization vector is -d_(al,mu)***
*************************************************
local amps = -([M1]+[M2]+[M3]+[M4])*([M1*]+[M2*]+[M3*]+[M4*])*
d_(al,mu);

************************************
*Dirac equation in momentum space***
************************************
id U(1,h?)*Ub(1,h?) = g_(1,h) + me*gi_(1);
id U(2,h?)*Ub(2,h?) = g_(2,h) + mm*gi_(2);

************************************
*Trace Calculating                ***
************************************
Trace4,1;
Trace4,2;
.sort

************************************
*On-shell condition               ***
************************************
id p1.p1 = me2;
id p2.p2 = mm2;
id p3.p3 = me2;
id p4.p4 = mm2;
id k.k   = 0;
*print amps;
.sort

repeat;
id k = p1 + p2 - p3 - p4;
id p1.p1 = me2;
id p2.p2 = mm2;
```

```
id p3.p3 = me2;
id p4.p4 = mm2;
endrepeat;
.sort

*************************************
*Change to convenient variables  ***
*************************************
id mm^4  = mm4;
id me^4  = me4;
id me^2  = me2;
id mm^2  = mm2;
id me2^2 = me4;
id mm2^2 = mm4;
id p1.p2 = d12;
id p2.p1 = d12;
id p1.p3 = d13;
id p3.p1 = d13;
id p1.p4 = d14;
id p4.p1 = d14;
id p2.p3 = d23;
id p3.p2 = d23;
id p2.p4 = d24;
id p4.p2 = d24;
id p3.p4 = d34;
id p4.p3 = d34;
format doublefortran;

*************************************
*Print result and format to fortran*
*************************************
print amps;
.end
```

BIBLIOGRAPHY

[1] U. Marconi, *The MUonE experiment*, *EPJ Web Conf.* **212** (2019) 01003.

[2] MUONE collaboration, G. Abbiendi, *Measurement of the leading hadronic contribution to the muon g-2 via space-like data*, *PoS* **EPS-HEP2017** (2017) 358.

[3] MUON G-2 collaboration, J. Grange et al., *Muon (g-2) Technical Design Report*, 1501.06858.

[4] J-PARC G-2 collaboration, T. Mibe, *Measurement of muon g-2 and EDM with an ultra-cold muon beam at J-PARC*, *Nucl. Phys. B Proc. Suppl.* **218** (2011) 242.

[5] E34 collaboration, Y. Sato, *Muon g-2/EDM experiment at J-PARC*, *PoS* **KMI2017** (2017) 006.

[6] Le Duc Truyen, Electron muon elastic scattering in one-loop QED with soft-photon corrections, Bachelor thesis (2020), http://ifirse.icise.vn/wp-content/uploads/2020/09/LeDucTruyen_bachelor_2020.pdf

[7] M. Alacevich, C. M. Carloni Calame, M. Chiesa, G. Montagna, O. Nicrosini and F. Piccinini, *Muon-electron scattering at NLO*, *JHEP* **02** (2019) 155 [1811.06743].

[8] S. Kawabata, *A New version of the multidimensional integration and event generation package BASES/SPRING*, *Comput. Phys. Commun.* **88** (1995) 309.

[9] G. P. Lepage, *Adaptive multidimensional integration: VEGAS enhanced*, *J. Comput. Phys.* **439** (2021) 110386 [2009.05112].

[10] G. P. Lepage, "Adaptive multidimensional monte carlo integration." https://github.com/gplepage/vegas, 2021.

[11] M. E. Peskin and D. V. Schroeder, *An Introduction to quantum field theory*. Addison-Wesley, Reading, USA, 1995.

[12] E. Byckling and K. Kajantie, *Particle Kinematics*. University of Jyvaskyla, Jyvaskyla, Finland, 1971.

[13] B. Ruijl, T. Ueda and J. Vermaseren, *FORM version 4.2*, 1707.06453.

[14] T. Hahn and M. Perez-Victoria, *Automatized one loop calculations in four-dimensions and D-dimensions*, *Comput. Phys. Commun.* **118** (1999) 153 [hep-ph/9807565].

[15] T. Hahn, *Generating Feynman diagrams and amplitudes with FeynArts 3*, *Comput. Phys. Commun.* **140** (2001) 418 [hep-ph/0012260].

[16] A. Lahiri and P. B. Pal, *A First Book of Quantum Field Theory*. 2005.

[17] W. H. Furry, *Lorentz transformation and the thomas precession*, *American Journal of Physics* **23** (1955) 517 [https://doi.org/10.1119/1.1934085].